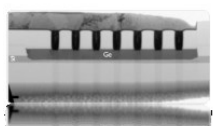
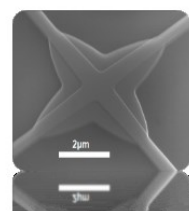
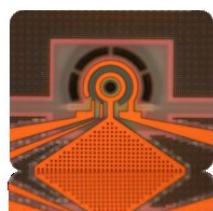




Library Handbook

ISIPP50G 2.3.0



Changes

Version	Change
X.Y.Z	See changelog document
1.0.1	Bug fixes release
1.0.0	Initial release

Contents

1	Document information	4
1.1	Purpose	4
1.2	Scope.....	4
1.3	Responsibility	4
2	Important information.....	5
3	Conventions.....	6
3.1	Cell format.....	6
3.2	Device Families	6
3.3	Maturity levels.....	6
3.4	Measurement details	6
4	ISIPP50G devices library.....	7
4.1	Waveguides	7
4.2	Transitions	15
4.3	Crossings.....	15
4.4	Fiber grating couplers	16
4.5	Multi-mode interferometers (MMI)	22
4.6	Directional coupler.....	25
4.7	Edge couplers.....	32
4.8	Templates	35
4.9	Bond pads	36
4.10	Contacts.....	37
4.11	50Ω Resistors	38
4.12	Thermo-optic phase shifter	39
4.13	PN depletion line phase shifter.....	40
4.14	Mach-Zehnder modulator (MZM)	45
4.15	Ring modulators	48
4.16	Ge Photodetectors.....	54
4.17	SiGe devices	62

I Document information

I.1 Purpose

The purpose of this document is to describe imec's silicon photonics ISIPP50G devices library and specifications to take into account when designing into ISIPP50G technology. The library consists of both O-band and C-band devices and circuits. These are characterized and tested components with varying levels of maturity to enable complex circuit designs and lower the threshold for access.

I.2 Scope

The devices library in ISIPP50G is intended to be useful for prototyping and manufacturing of devices for a wide range of applications, but with a focus on communication devices. The device parameters are fixed and cannot be altered by the customer.

I.3 Responsibility

It is the responsibility of the designer to make sure that their design is compatible with the processing. Imec cannot provide any guarantee that the device library circuit will have the functionality it was designed for.

2 Important information

With the ISIPP50G PDK release, Imec's silicon photonics technology is making a significant step forward to support component's performance for 50Gb/s operation.

At the same time there has been a change in the overall process integration to support faster turn-around time in the future with maintained quality. While performance matching with the older process has been demonstrated there is less historical data based on the upgraded flow. Therefore there is less statistical information compared to the ISIPP25G PDK although the process control is expected as good or better.

3 Conventions

3.1 Cell format

The devices from the library are provided as fixed GDSII cells. See the section *Using Library Cells* in the Layout Handbook for more information.

3.2 Device Families

Device Family	Acronym	Classes example
Waveguides	WG	Strip Waveguide C-Band TE (SWGCTE), Rib Waveguide O-Band TE polarization (RWGOTE)
Transitions	TRA	Waveguide transitions
Waveguide Crossing	X	Crossing C-Band TE polarization (XCTE)
Fiber Grating Couplers	FGC	Coupler C-Band TE polarization (FGCCTE), 2D grating coupler (FGCC)
Multi-Mode Interferometers	M	MMI 1X2 C-Band TE polarization (M12CTE)
Directional Couplers		
Edge coupler	FEC	Edge coupler C-band (FECC)
Templates	TEMPLATE	
Bond pads	BP	
Contact	CONTACT	
Resistors	R	
Heated waveguides	WGNPLUS	Heated Strip Waveguide C-Band (SWGCTE_WGNPLUS)
Phase Shifters	PS	Phase shifter plasma dispersion effect C-band TE (PSDCTE).
Mach-Zehnder Modulators	MZM	MZMCTE, MZMOTE
Ring Modulators	RM	Ring Modulator C-band TE polarization (GPDCTE)
Ge Photodetectors	GPD	Photodiode C-band TE polarization (GPDCTE)
Electro-Absorption Modulators	EAM	EAM C-band TE (EAMCTE)

3.3 Maturity levels

Devices in the library have been rated with a maturity level to indicate the level of testing/data available for the device. The maturity levels defined are:

- 0: simulations/ short loop measurement data/tested die level
- 1: limited wafer scale data
- 2: wafer scale testing on at least two wafers from different mask-sets

3.4 Measurement details

We use a standard single mode fiber with 9 µm core diameter and flat cleave. Typical fiber height above the grating is 20 µm and the fiber is aligned 10° off the vertical without any index matching liquid.

Unless otherwise stated, measurements for the specifications that are provided, have been performed at room temperature.

We report, where available, the statistics of the distribution of device specifications with the mean, median, the 10% and 90% quantiles (Q10 & Q90), the standard deviation (std dev) and the number of observations (N).

4 ISIPP50G devices library

4.1 Waveguides

4.1.1 Propagation losses

4.1.1.1 Test structure

We use a set consisting of four waveguides of a certain type with different total waveguide lengths. The waveguides are laid out as spirals to enable smaller footprint and straight forward testing (Figure 1). The impact of bending loss is minimized by choosing relaxed bending radii.

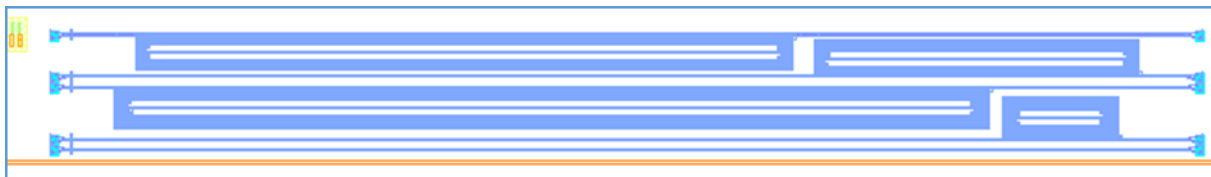


Figure 1: A typical set of four SWGCTE_WG_450 waveguides in the SOI platform. Lengths are 1, 2, 4 and 7cm, respectively. Bend radius is 10 μm .

4.1.1.2 Experiment

The transmission loss is determined by measuring the transmission spectrum of all the waveguide lengths. It is important that the spectral response of the fiber grating coupler is consistent and hence all waveguides are aligned at a fixed wavelength (e.g. C-band at 1550nm or O-band at 1310nm).

4.1.1.3 Analysis method

We use cut-back method to analyze the propagation loss. To normalize the measured spectra, a polynomial fit of the reference waveguide is used to remove the spectral shape of the grating couplers. The order of the polynomial depends on the shape of the grating coupler response and the selected wavelength range. Typically a fourth order polynomial is used.

The insertion loss (IL) at a given wavelength as a function of waveguide length is shown in Figure 2b. Note that the polynomial fit of the normalized spectra is used for this evaluation. From the slope of the linear regression of these transmission points, the waveguide loss is determined. The quality of the linear regression or fit is expressed with the regression factor R. In Figure 2b, the waveguide loss of 1.36dB/cm at 1550nm with a fitting quality of 0.9998 is obtained.

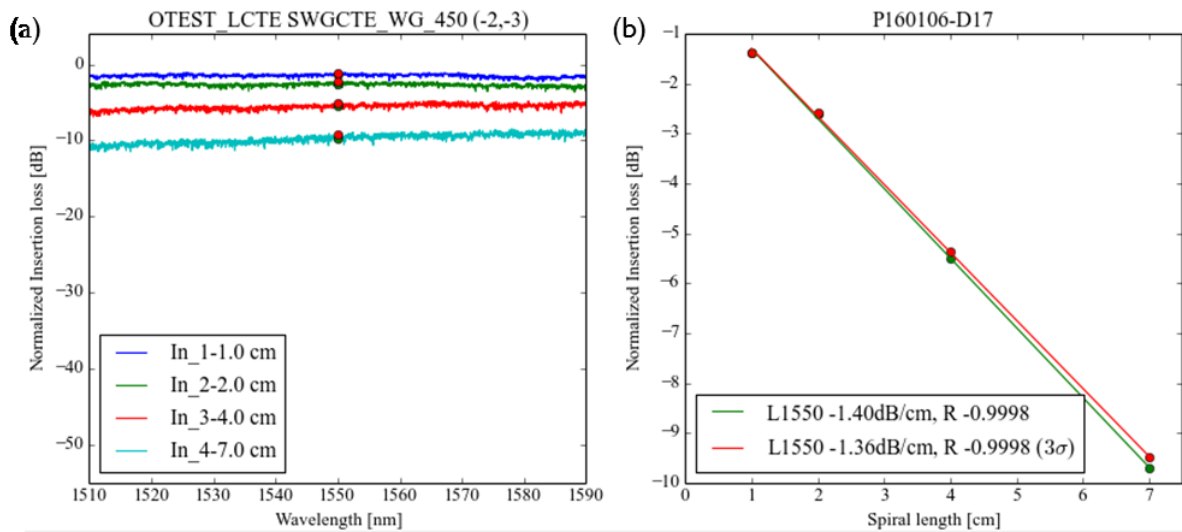


Figure 2: A typical analysis to determine the waveguide loss. In this example the strip waveguide SWGCTE_WG_450 has a propagation loss of 1.36dB/cm.

Larger than expected scattering or multi-mode effects in a bend can cause large dips in the spectral response due to destructive interference. This spectral noise can affect the polynomial fit of the normalized spectra which typically causes an overestimation of the insertion loss and hence propagation loss. A compensation based on the magnitude of the spectral noise is applied to the insertion loss which provides a better estimation of the propagation loss. This compensation is calculated based on the 3σ of the deviations of the spectrum with respect to the polynomial fit. This is annotated by 3σ in Figure 2b.

4.1.2 Phase and group velocity

The phase and group velocity is typically expressed as the effective refractive index (n_{eff}) and group index (n_g).

4.1.2.1 Test structure

The filter spectrum of a simple Mach-Zehnder interferometer (MZI) can be used to extract group velocity. A schematic of this MZI and a typical spectrum is shown in Figure 3.

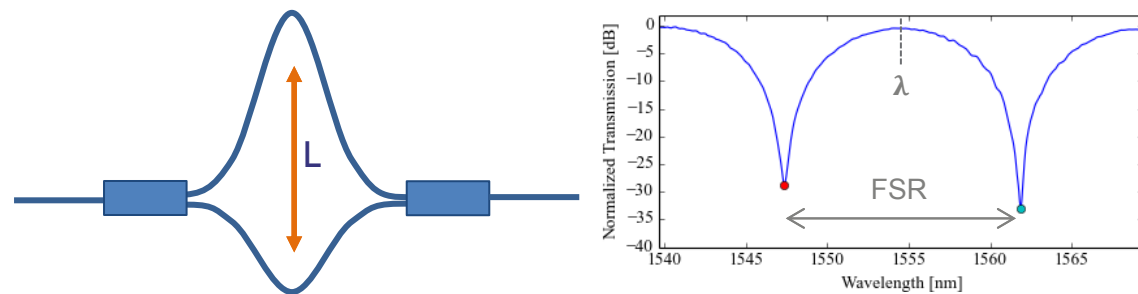


Figure 3 (left) A schematic overview of a MZI with length difference L between the two arms. This length difference determines the FSR. The measurement of the FSR (right) and the knowledge of L can be used to calculate n_g .

Based on the free-spectral range (FSR), the wavelength between the two spectral minima (λ) and the length difference L between the MZI arms, one can calculate n_g using following formula:

$$n_g = \frac{\lambda^2}{FSR * L} \quad (1)$$

The n_{eff} can be extracted using the wavelength of destructive interference (λ_{peak}), the length and the filter order m.

$$n_{eff} = \frac{\lambda_{peak} * m}{L} \quad (m = 1,2,3, \dots) \quad (2)$$

The filter order is the integer amount of times the light at wavelength λ_{peak} fits in the delay length L. This value is usually unknown but can be estimated based on the FEM-simulated value of n_{eff} for the given waveguide structure. The strip waveguide under consideration has assumed dimensions with width 450nm and height 215nm, resulting in an effective refractive index of 2.33 at 1550nm. Light at 1550nm will hence fit 60 times in this delay line.

Using this approach, the n_{eff} is only known at wavelengths that are determined by the wafer-level waveguide dimensional variation (i.e. at λ_{peak}) and not at a certain analysis wavelength (e.g. 1550nm). Furthermore it is found that local quasi-random waveguide dimensional variations can shift the phase of a MZI with approximately $\pi/10$ between neighbouring structures. To cope with both undesired variations, an array of eight MZIs is designed with a slightly different delay length ($L + n * \Delta L$). ΔL is chosen such that all eight channels are within one FSR ($\Delta L = FSR/(8+1)$). This causes the spectral dips to shift in wavelength ($\lambda + n * \Delta \lambda$). This approach has two benefits. First, it enables the extraction of the wavelength dependency of n_{eff} which allows the extraction of n_{eff} on a certain analysis wavelength, independent on the exact peak wavelength (λ_{peak}). Due to this fitting of the eight independent structures, the effect of local variations can be minimized.

The FSR is 14.1 nm which is determined by the length difference L of 40 um. The relative length difference ΔL is designed to be 71.5nm with an expected wavelength shift of 1.6 nm. The input and output splitters are respectively a 1x2 and 2x1 MMI. This test site is shown in Figure 4.

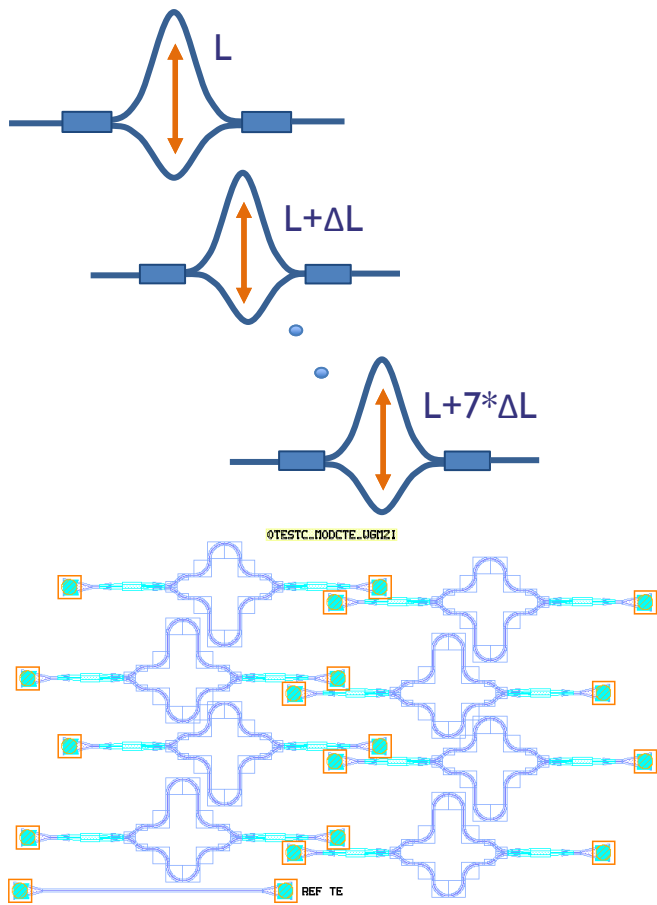


Figure 4: The test site to extract the n_{eff} and ng consist of eight MZIs to minimize the local variability due to dimensional variations.

4.1.2.2 Analysis

A typical spectral analysis is shown in Figure 5. The eight spectral minima under analysis are chosen based on their relative position to the target wavelength (i.e. 1550 nm). The optimal linear regression between the wavelength of the eight spectral minima as function of device number is shown in Figure 5 (right) which shows the effect of local waveguide dimensional variation. The local group index is calculated as the mean value of the eight MZIs and has a value around 4.26.

n_{eff} is calculated for the eight MZIs separately using the same filter order and are then fitted to a second order polynomial. This fitting is then evaluated at the target wavelength (i.e. 1550nm). In this case n_{eff} is 2.3455, which agrees with FEM simulations.

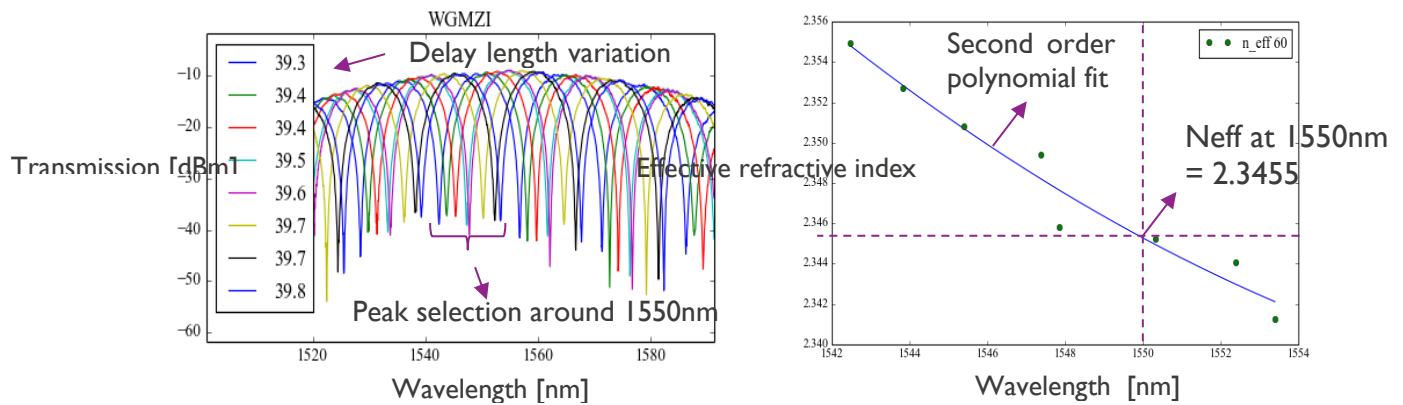


Figure 5: A typical analysis for the extraction of n_{eff} .

4.1.3 Strip waveguide C-band

DEVICE	SWGCTE_WG_450									
Family	Waveguide			SWGCTE_WG_450_10k.gds						
Class	Strip Waveguide			Maturity Level		2				
Type	Fully etched waveguide (WG), C-band TE polarization									
STRUCTURAL					Values				Unit	
	GDS		Q90		Mean	Q10				
DIM1 Waveguide Core Width				450		480				nm
DIM2 Waveguide Cladding Width				2000						nm
FUNCTIONAL At 1550nm	Specification			Extracted values						Unit
	Min	Target	Max	Median	Mean	Std	Q90	Q10	N	
SPEC1 Propagation Loss TE		1.6	2	1.4		0.2	1.64	1.21	751	dB/cm
SPEC2 Effective index TE		2.33		2.31						
SPEC3 Group index TE		4.26		4.23		0.017	4.206	4.252	42	
SPEC4 Propagation Loss TM				0.8						

4.1.4 Strip waveguide O-band

DEVICE	SWGOTE_WG_380									
Family	Waveguide			SWGOTE_WG_380_10k.gds						
Class	Strip Waveguide			Maturity Level		2				
Type	Fully etched waveguide (WG), O-band TE polarization									
STRUCTURAL					Values				Unit	
	GDS		Q90		Mean	Q10				
DIM1 Waveguide Core Width				380						nm
DIM2 Waveguide Cladding Width				2000						nm
FUNCTIONAL At 1310nm	Specification			Extracted values						Unit
	Min	Target	Max	Median	Mean	Std	Q90	Q10	N	
SPEC1 Propagation Loss TE		3	3.5	2.6		0.26	2.36	2.93	212	dB/cm
SPEC2 Effective index TE										
SPEC3 Group index TE										
SPEC4 Propagation Loss TM				1.2						

4.1.5 SKT rib waveguide C-band

DEVICE	RWGCTE_SK_450								
Family	Waveguide			RWGCTE_SK_450_10k.gds					
Class	Rib Waveguide			Maturity Level		2			
Type	Partially etched waveguide (SKT), C-band TE polarization								
STRUCTURAL					Values				Unit
					GDS	Q90	Mean	Q10	
DIM1 Waveguide Core Width				450		490			nm
DIM2 Waveguide Cladding Width				4000					nm
FUNCTIONAL At 1550 nm	Specification			Extracted values					
	Min	Target	Max	Median	Mean	Std	Q90	Q10	N
SPEC1 Propagation Loss TE				1.0		0.2	1.89	0.86	751
SPEC2 Effective index TE									
SPEC3 Group index TE									

4.1.6 SKT rib waveguide O-band

DEVICE	RWGOTE_SK_380								
Family	Waveguide			RWGOTE_SK_380_10k.gds					
Class	Rib Waveguide			Maturity Level		1			
Type	Partially etched waveguide (SKT), O-band TE polarization								
STRUCTURAL					Values				Unit
					GDS	Q90	Mean	Q10	
DIM1 Waveguide Core Width				380					nm
DIM2 Waveguide Cladding Width				4000					nm
FUNCTIONAL At 1310 nm	Specification			Extracted values					
	Min	Target	Max	Median	Mean	Std	Q90	Q10	N
SPEC1 Propagation Loss TE				2.25		0.3	2.7	1.91	303
SPEC2 Effective index TE									
SPEC3 Group index TE									

4.1.7 FC rib waveguide C-band

DEVICE	RWGCTE_FC_650											
Family	Waveguide			RWGCTE_FC_650_10k.gds								
Class	Rib Waveguide			Maturity Level		I						
Type	Shallow etched waveguide (FC), C-band TE polarization											
STRUCTURAL				Values				Unit				
				GDS	Q90	Mean	Q10					
DIM1 Waveguide Core Width				650				nm				
DIM2 Waveguide Cladding Width				4000				nm				
FUNCTIONAL At 1550nm	Specification			Extracted values								
	Min	Target	Max	Median	Mean	Std	Q90	Q10	N			
SPEC1 Propagation Loss TE				0.6		0.2	0.87	0.46	988			
SPEC2 Effective index TE												
SPEC3 Group index TE												

4.1.8 FC rib waveguide O-band

DEVICE	RWGOTE_FC_580											
Family	Waveguide			RWGOTE_FC_580_10k.gds								
Class	Rib Waveguide			Maturity Level		I						
Type	Shallow etched waveguide (FC), O-band TE polarization											
STRUCTURAL				Values				Unit				
				GDS	Q90	Mean	Q10					
DIM1 Waveguide Core Width				580				nm				
DIM2 Waveguide Cladding Width				4000				nm				
FUNCTIONAL At 1310 nm	Specification			Extracted values								
	Min	Target	Max	Median	Mean	Std	Q90	Q10	N			
SPEC1 Propagation Loss TE				0.7		0.1	0.86	0.59	304			
SPEC2 Effective index TE												
SPEC3 Group index TE												

4.2 Transitions

A cut-back method is used to characterize the maximum insertion loss of transitions across the band.

Device Name	Structure	Par	Q10	Mean	Q90	Std dev	Unit	Mat	N
C-Band Devices									
TRACTE_WGFC_450_650	SWGCTE_WG_450 to RWGCTE_FC_650	Insertion loss		0.02			dB	I	
TRACTE_WGSK_450_450	SWGCTE_WG_450 to RWGCTE_SK_450	Insertion loss		0.007			dB	I	
O-Band Devices									
TRAOTE_WGFC_380_580	SWGCTE_WG_380 to RWGCTE_FC_580	Insertion loss		0.008			dB	I	
TRAOTE_WGSK_380_380	SWGOTE_WG_380 to RWGOTE_SK_380	Insertion loss		0.007			dB	I	

4.3 Crossings

A cut-back method is used to characterize the maximum insertion loss of waveguide crossing across the band.

Device Name	Structure	Par	Q10	Medi an	Q90	Std dev	Unit	Mat	N
C-Band Devices									
XCTE_FCWG_764_2080	Waveguide crossing	Insertion loss	0.23	0.28	0.36	0.05	dB	2	122
		Cross-talk	-30	-31.7	-34.6	1.7	dB		
O-Band Devices									
XOTE_FCWG_647_1775	Waveguide crossing	Insertion loss		0.6			dB	I	
		Cross-talk	-30	-31			dB		

4.4 Fiber grating couplers

The fiber grating coupler is used to couple the light from a fiber into the integrated circuit and vice-versa. The most common performance metrics of a fiber grating coupler (FGC) are the peak insertion loss (IL_p), spectral bandwidth (BW_{1dB}) and the peak wavelength (λ_{center}).

4.4.1 Characterization method

4.4.1.1 Test structure

The test structure used to characterize the fiber grating coupler is a short, straight waveguide with two identical fiber grating couplers as input and output. An example is shown in Figure 6, where two FGC are tested respectively for TM and TE polarization.



Figure 6: Test structure for the characterization of a fiber grating coupler.

4.4.1.2 Measurement method

To obtain equal spectral response between the input and output FGC, it is necessary that the input and output fibers have the same height above the grating and the same fiber angle with respect to the grating under test. We first align the fiber in X-Y at the expected peak wavelength. From this initial measurement the actual wavelength is extracted. A second X-Y alignment is done at this extracted peak wavelength. The fiber height (Z) is nominally fixed at 20um. No index-matching fluid is used.

4.4.1.3 Analysis method

It is important for the accuracy of the IL spectrum that the IL of the external circuit (e.g. polarization rotator and others) is known. The IL of the external circuit is measured by optically shorting the DUT with a pigtail. With this data, the measured spectrum is referenced to achieve the Fiber-to-Fiber IL spectrum as shown in Figure 7.

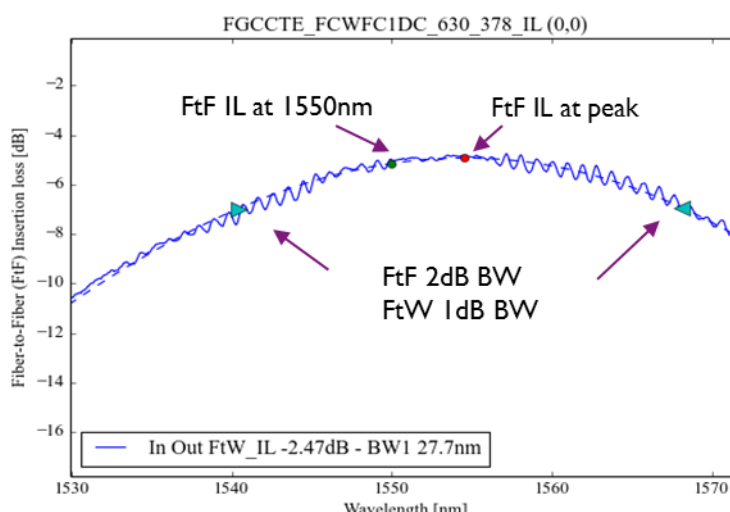


Figure 7: A typical Fiber-to-Fiber spectrum of FGCTE_FCWFIDC. The Fiber-to-Waveguide (FtW) peak IL is -2.47 dB, the λ_{center} is 1555 nm and the FtW 1dB bandwidth (BW1dB) is 27.7 nm.

To lower the influence of possible unintended reflections between the FGCs or between the FGC and the fiber, a fourth-order polynomial fit is used. The maximum of that fit is used to determine the peak Fiber-to-Fiber insertion loss (FtF IL) and the center wavelength (λ_{center}). As shown in Figure 7, the λ_{center} is slightly different than the target wavelength (1550nm). The Fiber-to-Waveguide (FtW) IL can be estimated by dividing the FtF IL estimate by two. Similarly, we use the FtF IL spectrum to estimate the bandwidth (BW) of the FGC. Therefore, the 2dB FtF BW is extracted from the FtF spectrum, which is representative of the FtW 1dB BW. From Figure 8, the FtW IL is estimated to be -2.47 dB, the λ_{center} 1555 nm and the 1dB FtW BW 27.7 nm.

4.4.2 Device performances

The PDK grating couplers thereafter are designed for coupling to SMF-28 fiber, thus 10.4 μm MFD @ 1550 nm, 9.2 μm MFD @ 1310. Furthermore, these are designed and tested for fibers with perpendicular (0° cleave) facets oriented at 10° in air. This is equivalent to fiber blocks polished at about 6.9° .

C-band	O-band
FGCCTE_FCIDC_625_313	FGCOTE_FCIDC_489_245
FGCCTE_FCWFCIDC_630_378	FGCOTE_FCWFCIDC_500_325
FGCCTM_FCIDC_984_492	FGCOTM_FCIDC_720_396
FGCC_2DC_600_390	

4.4.2.1 C-band

DEVICE	FGCCTE_FCIDC_625_313									
Family	Fiber Grating Coupler			FGCCTE_FCIDC_625_313.gds						
Class	TE Polarization, C-band			Maturity Level		I				
Type	Shallow etched grating coupler (FC), one-dimensional, curved									
STRUCTURAL				Values				Unit		
				GDS	Q90	Mean	Q10			
DIM1 Grating Pitch	325					625		nm		
DIM2 Grating Trench Width	313							nm		
FUNCTIONAL At 1550nm	Specification			Extracted values					Unit	
	Min	Target	Max	Median	Mean	Std	Q90	Q10	N	
SPEC1 Peak Insertion Loss IL_p				-4.3		0.4	-4.7	-3.7	56	dB
SPEC2 Peak Wavelength λ_{center}				1558.0		20.6	1559.7	1555.4	56	nm
SPEC3 Fiber to Waveguide 1-dB Bandwidth BW_{1dB}				28.5		1.3	30.8	27.1	56	nm

DEVICE	FGCCTE_FCWFCIDC_630_378								
Family	Fiber Grating Coupler					FGCCTE_FCWFCIDC_630_378.gds			
Class	C-band, TE Polarization					Maturity Level	I		
Type	Poly-silicon (FCW) and shallow etched grating coupler (FC), one-dimensional, curved								
STRUCTURAL				Values					Unit
				GDS	Q90	Mean	Q10		
DIM1 Grating Pitch	630					630			nm
DIM2 Grating Trench Width	378								nm
FUNCTIONAL At 1550nm	Specification			Extracted values					
	Min	Target	Max	Median	Mean	Std	Q90	Q10	N
SPEC1 Peak Insertion Loss IL_p				-2.4		0.4	-2.9	-1.9	56
SPEC2 Peak Wavelength λ_{center}				1564.1		3.3	1569	1560.6	56
SPEC3 Fiber to Waveguide 1-dB Bandwidth BW_{1dB}				35.2		5.6	43.7	30.3	56

DEVICE	FGCCTM_FCIDC_984_492								
Family	Fiber Grating Coupler					FGCCTM_FCIDC_984_492.gds			
Class	C-band, TM Polarization,					Maturity Level	I		
Type	Shallow etched grating coupler (FC), one-dimensional, curved								
STRUCTURAL				Values					Unit
				GDS	Q90	Mean	Q10		
DIM1 Grating Pitch	984								nm
DIM2 Grating Trench Width	492								nm
FUNCTIONAL At 1550nm	Specification			Extracted values					
	Min	Target	Max	Median	Mean	Std	Q90	Q10	N
SPEC1 Peak Insertion Loss IL_p				-4.9					14
SPEC2 Peak Wavelength λ_{center}				1553.9					14 nm
SPEC3 Fiber to Waveguide 1-dB Bandwidth BW_{1dB}				35.1					14 nm

DEVICE	FGCC_2DC_600_390									
Family	Fiber Grating Coupler			FGCC_2DC_600_390.gds						
Class	C-band, polarization independent			Maturity Level	I					
Type	Shallow etched grating coupler (FC), two-dimensional, curved, TE polarization as output.									
STRUCTURAL				Values						
				GDS	Q90	Mean	Q10		Unit	
DIM1 Grating Pitch	600								nm	
DIM2 Grating hole diameter	390								nm	
FUNCTIONAL At 1550nm	Specification			Extracted values					Unit	
	Min	Target	Max	Median	Mean	Std	Q90	Q10	N	
SPEC1 Peak Insertion Loss IL_p		-6								dB
SPEC2 Peak Wavelength λ_{center}		1550								nm
SPEC3 Fiber to Waveguide 1-dB Bandwidth BW_{1dB}		30								nm

4.4.2.2 O-band

DEVICE	FGCOTE_FCIDC_489_245									
Family	Fiber Grating Coupler, O-band TE			FGCOTE_FCIDC_489_245						
Class	O-band, TE polarization			Maturity Level	I					
STRUCTURAL	Values								Unit	
	GDS	Q90	Mean	Q10						
DIM1 Grating Pitch	489								nm	
DIM2 Grating Trench Width	245								nm	
FUNCTIONAL At 1310nm	Specification			Extracted values						
	Min	Target	Max	Median	Mean	Std	Q90	Q10	N	
SPEC1 Peak Insertion Loss IL _p				-3.39	-3.39	0.13	-3.55	-3.11	11	dB
SPEC2 Peak Wavelength λ _{center}				1304.7	1304.5	0.6	1303.4	1305.3	11	nm
SPEC3 Fiber to Waveguide 1-dB Bandwidth BW _{1dB}				24.6	24.8	1.3	23	26.5	11	nm

DEVICE	FGCOTE_FCWFIDC_500_325									
Family	Fiber Grating Coupler			FGCOTE_FCWFIDC_500_325.gds						
Class	O-band, TE polarization			Maturity Level	I					
STRUCTURAL	Values								Unit	
	GDS	Q90	Mean	Q10						
DIM1 Grating Pitch	500								nm	
DIM2 Grating Trench Width	325								nm	
FUNCTIONAL At 1310nm	Specification			Extracted values						
	Min	Target	Max	Median	Mean	Std	Q90	Q10	N	
SPEC1 Peak Insertion Loss IL _p				-2.51	-2.57	0.33	-3.24	-2.16	11	dB
SPEC2 Peak Wavelength λ _{center}				1308.5	1308.2	1.4	1306	1309.4	11	nm
SPEC3 Fiber to Waveguide 1-dB Bandwidth BW _{1dB}				20.8	20.7	0.45	19.9	21.4	11	nm

4.5 Multi-mode interferometers (MMI)

The MMIs in the library are designed to act as broadband power splitters or combiners. The MMI has either one input (a 1x2 MMI) or two inputs (a 2x2 MMI). The key performance parameters are the power splitting ratio, expressed as the power imbalance between the two outputs and the excess loss. This excess loss is defined as the extra loss apart from the intended power split.

4.5.1 Characterization method

4.5.1.1 Test structure

In Figure 8, the layout of the test structure to investigate the power splitting ratio of 1x2 MMI and 2x2 MMI are shown.

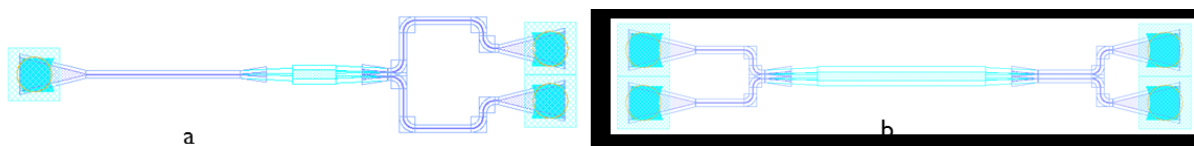


Figure 8: The layout of the test structure to test the power splitting ratio and IL of (a) a 1x2 MMI (b) a 2x2 MMI.

4.5.1.2 Measurement method

To investigate these test structures, the transmission spectrum of each input and output combination is measured and referenced with respect to a short reference waveguide structure to remove the spectral shape of the fiber grating couplers. The fiber alignment is performed at a fixed wavelength of interest (for C-band devices at 1550nm and for O-band devices at 1310m).

4.5.1.3 Analysis method

For the analysis of test structures (a) and (b), each spectrum is fit to a fourth order polynomial. A typical spectrum of a 1x2 MMI is shown in Figure 9. The analysis is carried out in a wavelength band of 40 nm around the wavelength of interest (e.g. for C-band devices: 1530 nm to 1570 nm).

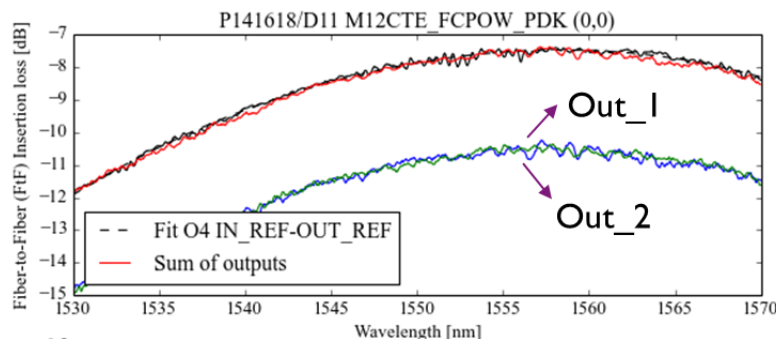


Figure 9: A typical spectrum and analysis of the 1x2 MMI library component.

In the spectrum from the reference waveguide (black curve) and the two output ports (green and blue curve) is shown. The two output ports have ~3 dB lower transmission than the reference waveguide. To assess the excess loss, both outputs are added together.

The *power imbalance*, defined as the power difference between the output ports is shown together with the two output spectra in Figure 10. From this 40 nm wide power imbalance spectrum, the mean power imbalance is calculated and shown as a red dashed line. In this example the mean power imbalance is practically 0 dB. The minimum and maximum of the power imbalance are shown as a black dashed line. The maximum of the absolute power imbalance is reported and is in this example around 0.4 dB.

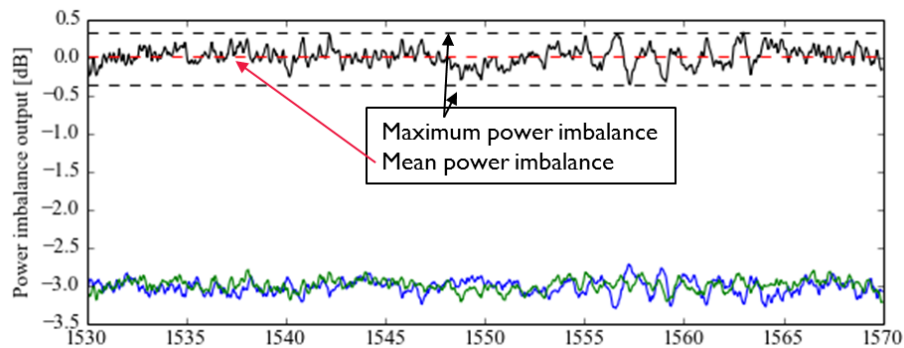


Figure 10: A typical power imbalance spectrum (black), with the 40 nm mean power imbalance indicated with a red dashed line as well as the maximum positive and negative power imbalance.

To assess the *excess loss*, a similar analysis is performed between the reference waveguide and the sum of the two outputs. This analysis is shown in Figure 11, where again the mean, minimum and maximum of the excess loss spectrum are calculated. In this example spectrum, the mean excess loss is 0.08 dB (red dashed line) and the maximum excess loss is 0.4 dB (around 1565 nm).

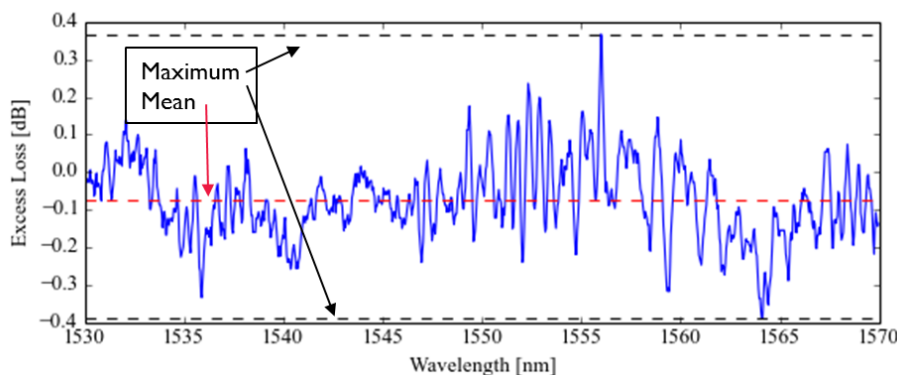


Figure 11: Excess loss spectrum with the 40 nm mean excess loss indicated by a red dashed line and the minimum and maximum with black dashed line.

4.5.2 Device performance

Device Name	Structure	Par	Spec	Q10	Mean	Q90	Std dev	Unit	Mat	N
C-Band Devices										
M12CTE_FC_50 00_25400	IX2 MMI for Quasi-TE mode	Excess Loss	Mean 40nm		0.04	0.13	0.1	dB		94
			Max 40nm							
	2X2 MMI for Quasi-TE mode	Power Imbalance	Mean 40nm		0.02	0.14	0.1	dB		
			Max 40nm							
M22CTE_FC_50 00_99800	2X2 MMI for Quasi-TE mode	Excess Loss	Mean 40nm					dB		
			Max 40nm							
		Power Imbalance	Mean 40nm					dB		
			Max 40nm							
		Phase accuracy			5%					
O-Band Devices										
M12OTE_FC_45 00_25600	IX2 MMI for Quasi-TE mode	Excess Loss	Mean 40nm					dB		
			Max 40nm							
	2X2 MMI for Quasi-TE mode	Power Imbalance	Mean 40nm					dB		
			Max 40nm							
M22OTE_FC_45 00_102400	2X2 MMI for Quasi-TE mode	Excess Loss	Mean 40nm					dB		
			Max 40nm							
		Power Imbalance	Mean 40nm					dB		
			Max 40nm							
		Phase accuracy			5%					

4.5.3 Discussion

M12

The M12CTE_FC_5000_25400 and M12OTE_FC_4500_25600 are working as expected, with a very low excess loss. This low excess loss makes it difficult to characterize accurately with the current test site. The mean power imbalance of the 40 nm wavelength window is 0 dB which indicates that the component behaves as expected. However, at some wavelengths the power imbalance reaches up to 0.55 dB.

M22

The 2X2 MMI has higher excess loss variability to the IX2 MMI. Since the component is typically 4 times longer than the IX2 MMI, the component can be expected to be less tolerant to fabrication variations. The excess loss for M22CTE_FC_5000_99800 can be as large as 1.1 dB for the shorter wavelengths (i.e. at 1530 nm) but can become very low for longer wavelengths (i.e. at 1570 nm). For M22OTE_FC_4500_102400 the largest excess loss is at longer wavelength (i.e. 1330 nm), whereas the low excess region is at shorter wavelengths (i.e. at 1290 nm). Both components have similar behaviour regarding power imbalance with respect to the IX2 MMIs.

4.6 Directional coupler

Directional coupling is defined as the power transfer between two neighbouring waveguides. The field coupling k is sinusoidal in function of coupling length. When the two waveguides are symmetric (same cross section), total power transfer ($K = 1$) can be reached. In this section we will quantify the coupling strength κ [$1/\mu\text{m}$] between two straight Si strip waveguides (SWG) and the coupling between two bending SWGs (κ_0) as shown in Eq. (3). It is important to note that the longer the wavelength, the larger the coupling strength is between the waveguides, due to a smaller confinement in the Si waveguide. Therefor all parameters are wavelength dependent.

$$\begin{aligned} K(\lambda) &= k(\lambda)^2 \\ &= \sin^2(\kappa(\lambda) * L_c + \kappa_0(\lambda)) \quad (3) \end{aligned}$$

Total power transfer is then reached when

$$L_c = \frac{\frac{\pi}{2} - \kappa_0(\lambda)}{\kappa(\lambda)} \quad (4)$$

4.6.1 Characterization method

4.6.1.1 Test structure

A Mach-Zehnder interferometer (MZI) with a varying input coupling (the directional coupler under test) and a fixed 3dB MMI combiner is used to extract the directional coupling and is shown in Figure 12. Depending on the input coupling ratio of the direction coupler, light will interfere differently at the output MMI which will be visible in the extinction ratio (ER) of the interference pattern. E.g. when the input power coupling is 50%, total destructive interference occurs with a large ER. When all the light is transferred from one waveguide to the other, no interference pattern is visible. In other words, the ER is zero.

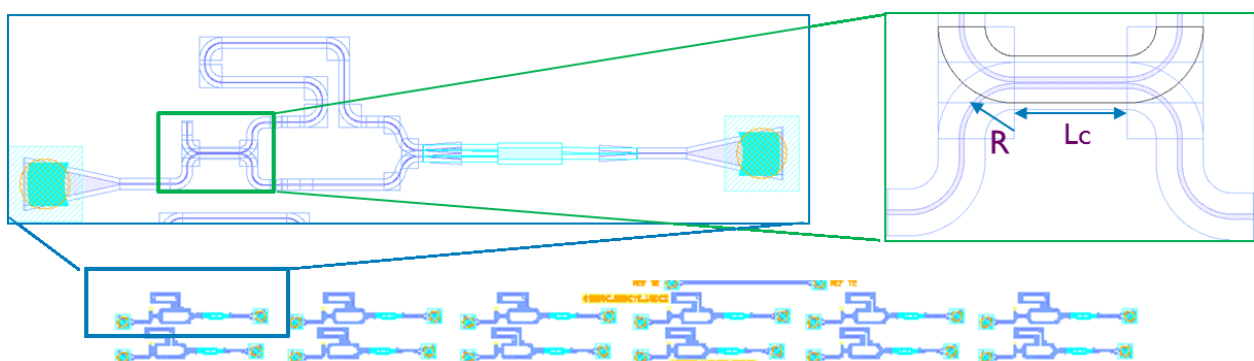


Figure 12: 12 test structures with varying coupling length (L_c) and fixed gap and radius R are used to extract the sinusoidal behaviour of directional coupling.

The test site to extract the directional coupling for a certain waveguide configuration consist of the same MZI structure but a varying coupling length (L_c). The radius R is equal to 5um and the waveguide gap is 150nm.

Two different regimes can be distinguished: the under-coupled regime where the longer the coupling length, the larger the power transfer and the over-coupled regime, where the coupling length is larger than the 100% coupling length. Increasing the coupling length will decrease the power transfer. In total 12 structures are designed to extract the sinusoidal trend of the power coupling in function of L_c and is varied between 0 and 20um. This is shown in Figure 13.

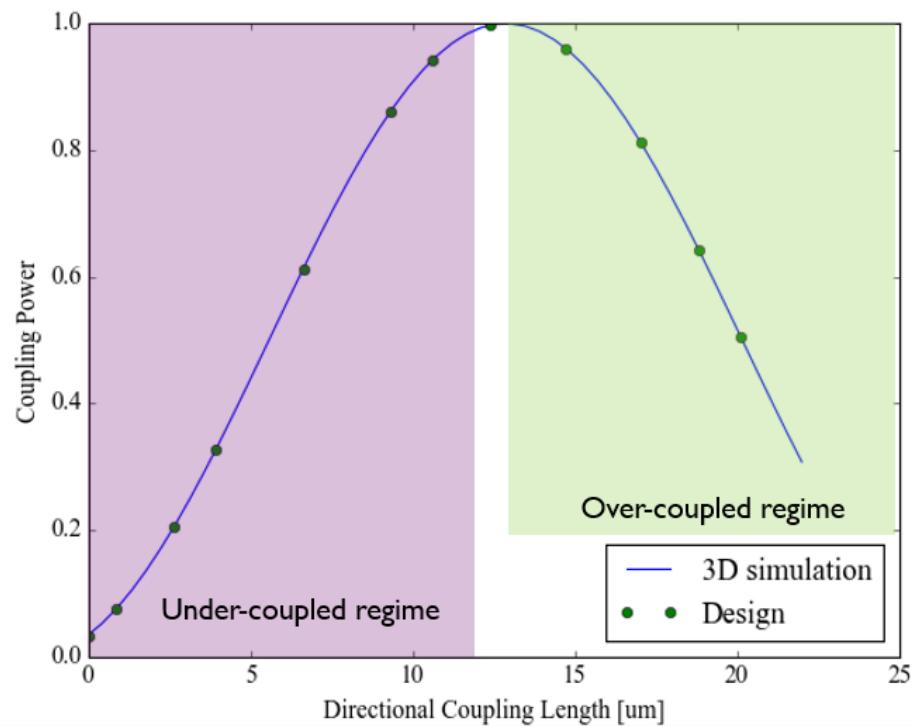


Figure 13: The simulated power transfer between two SWGs (gap 150nm, width 450nm, R 5um, oxide cladding at 1550nm) behaves as a sinus in function of coupling length. 12 structures are designed in such a way that a good sinusoidal fitting can be made.

4.6.1.2 Measurement method

Each structure is measured by acquiring the spectrum around the wavelength of interest. The advantage of using a MZI structure is its independency of the exact fiber alignment since the power coupling information is transferred to the spectral shape of the DUT.

4.6.1.3 Analysis method

One can calculate the local extinction ratio (ER) of an interference pattern as the difference between the local maximum and minimum. For each FSR ($= 4$ nm), this ER can be calculated such that an ER spectrum can be calculated. Using the matrix formalism one can easily deduct an analytical expression for the ER in function of the input coupling k :

$$ER_{dB} = 10 \log \left(\frac{\frac{1}{2} - k\sqrt{1-k^2}}{\frac{1}{2} + k\sqrt{1-k^2}} \right) \quad (5)$$

One can solve this equation to the field coupling k which gives two possible solutions in function of ER:

$$k_{\pm}^2 = K_{\pm} = \frac{1}{2} \pm \frac{1}{2} \sqrt{1 - \left(\frac{ER - 1}{ER + 1} \right)^2} \quad (6)$$

A typical analysis is shown in Figure 14. In Figure 14a, the spectrum of the test structure with $Lc = 17\text{um}$ is shown where all the local maxima and minima are indicated with a dot. For each min-max couple one can calculate the local ER and build an ER spectrum which is shown in Figure 14b. This ER spectrum can then be fitted with Eq. (5). Each ER data point has two solutions for K which are both shown in Figure 14c with respectively red and green dots. The correct solution for each wavelength must be picked based on the expected coupling and is different for each structure.

For this example Lc is 17um and hence we are in the over-coupled regime. In other words, the longer Lc the smaller the net power transfer. Hence, for the shortest wavelengths around 1520nm , the net power coupling is around 0.9um . For longer wavelengths around 1605nm the coupling strength is much larger and hence the coupling is in the far over-coupled regime (where only 20% of the power is transferred). The correct solutions are indicated with a purple region. The correct solutions for the power coupling in function of wavelength of Figure 14c is fitted to a sinusoidal function. Based on this fitting one can evaluate the power coupling for a user-defined set of wavelengths. This analysis is automated and repeated for all 12 structures.

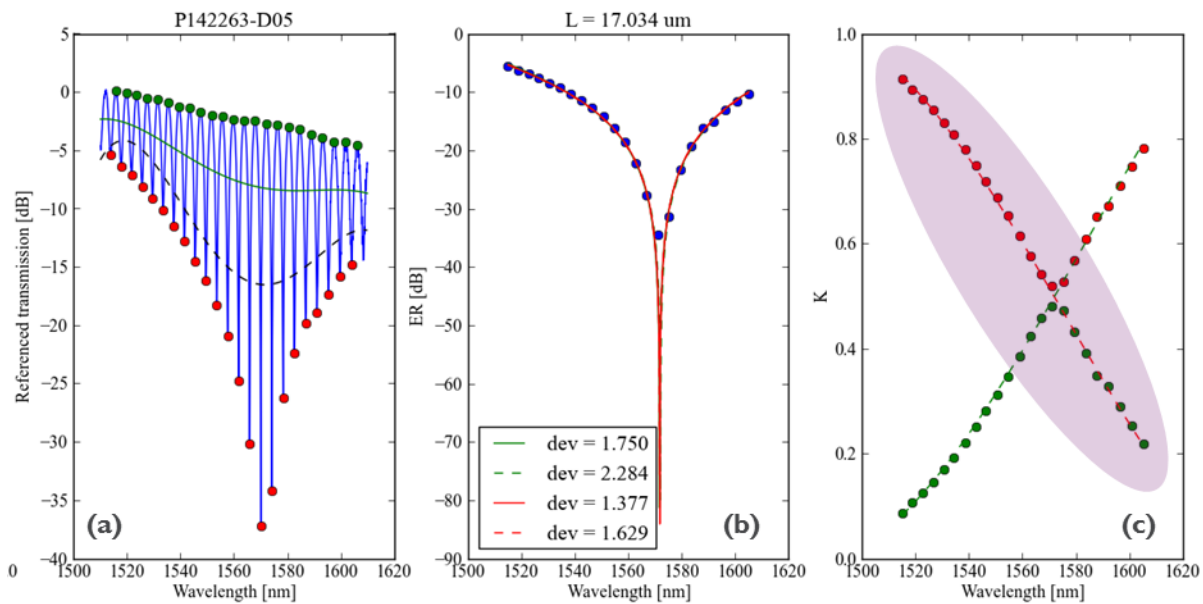


Figure 14: A typical spectral analysis to extract the directional coupling. The interference pattern (a) is characterized by an ER spectrum (b). This ER spectrum has for each data point two solutions for the power coupling (κ). The correct solution (within the purple area) can be picked for each wavelength based on the expected coupling.

In Figure 15, the power coupling in function of L_c at these user-defined set of wavelengths is plotted. One can find that indeed the coupling strength is larger for longer wavelengths and hence increases the frequency of power transfer. At $L_c = 0$, the remaining coupling is the coupling coming from the two bend sections.

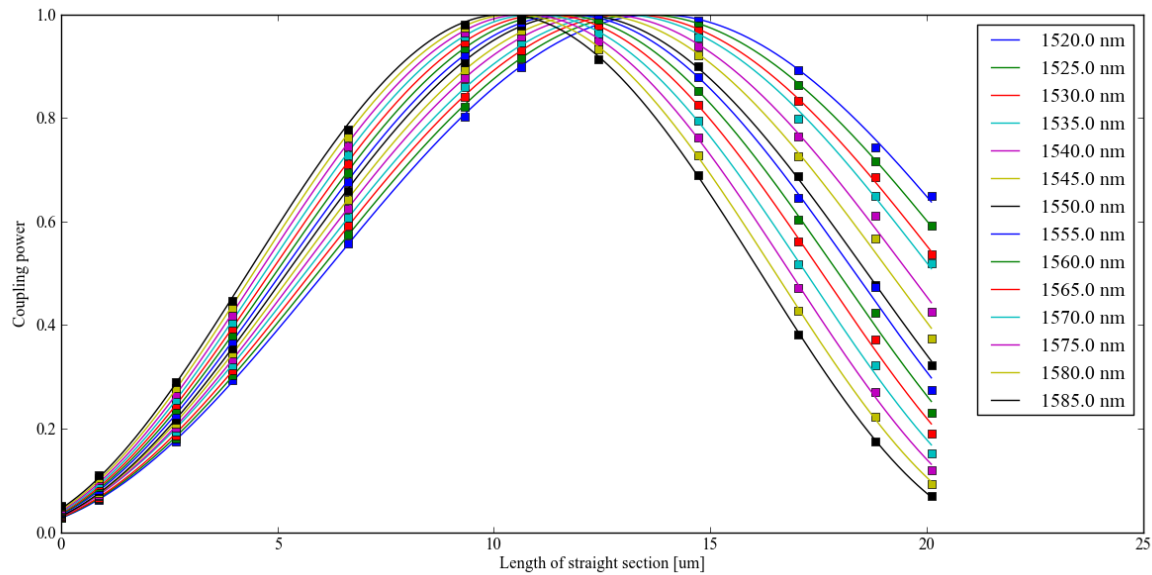


Figure 15: Power coupling in function of coupling length for a set of user-defined set of wavelengths.

For each wavelength, K can be fitted to the sinusoidal function of Eq. (3) with κ and κ_0 . These fitting parameters can be plotted in function of wavelength as shown in Figure 16. On top of these data, the 3D FDTD simulated values for the κ and κ_0 in function of wavelength. A very good agreement between extracted and simulated data is found.

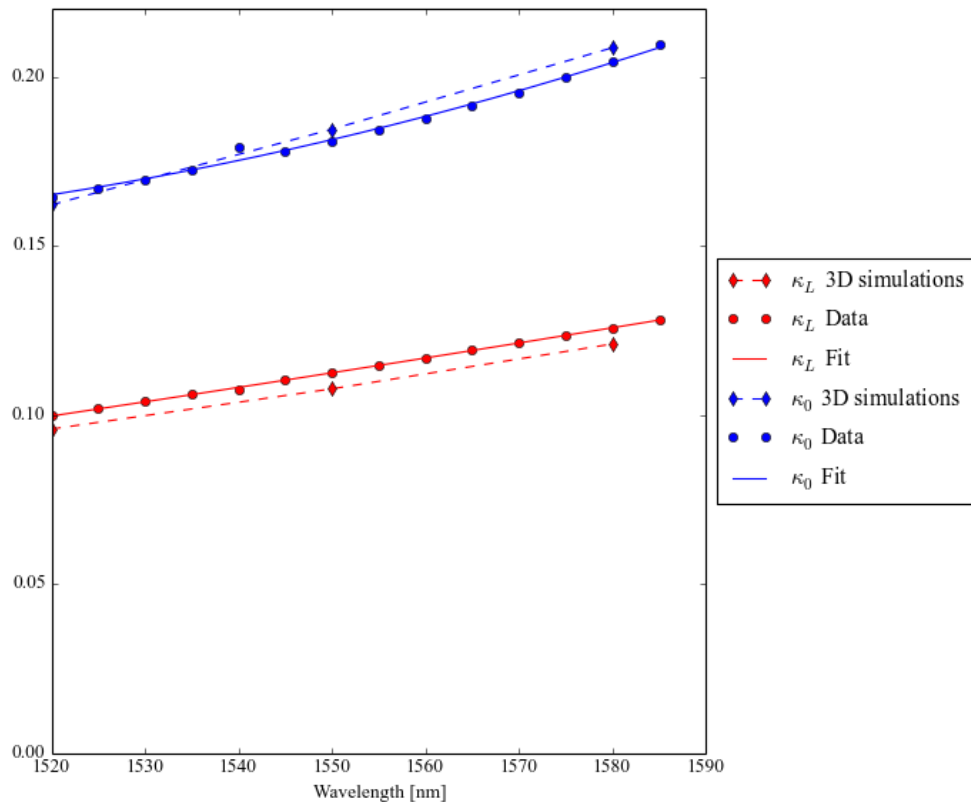


Figure 16: This figures shows the extracted fitting parameters κ (in $1/\mu\text{m}$ and with red dots) and κ_0 (blue dots) in function of wavelength together with the 3D FDTD simulated values.

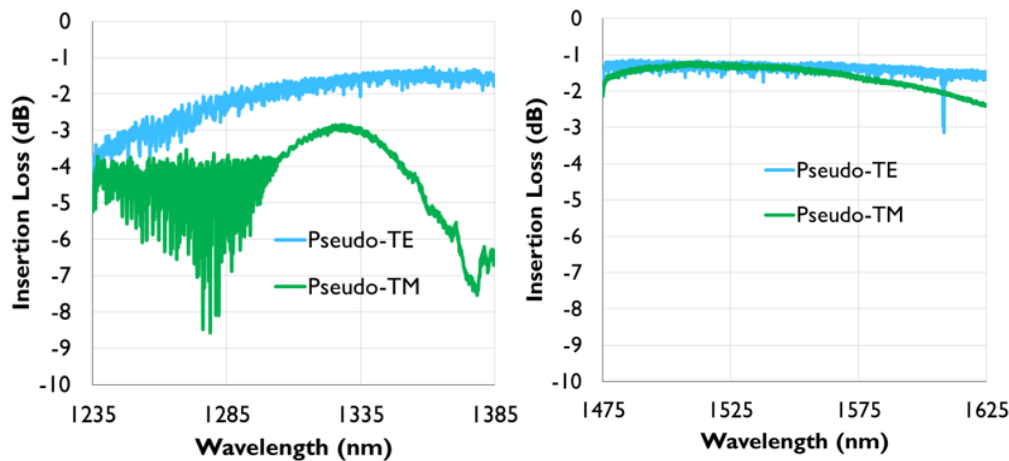
4.6.2 Device performance

The statistics for coupling strength κ and κ_0 (see eq.(3)) are reported for several wafers and mask sets. Around 14 dies, uniformly spread of the wafer are used to get a good within wafer uniformity.

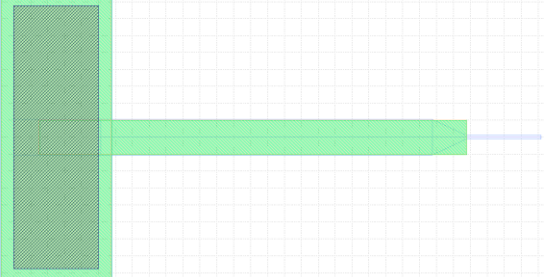
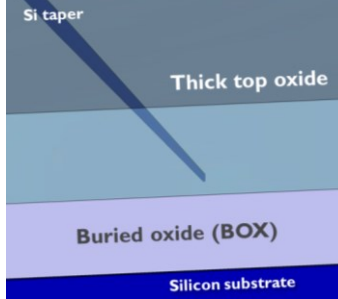
DEVICE	DCCTE_WG_450_150_5									
Family	Waveguide									
Class	Strip Waveguide, C-band, TE polarization									
Type	Fully etched waveguide (WG)									
Maturity Level	2									
GDS Filename										
STRUCTURAL				Values					Unit	
				GDS	Q90	Mean	Q10			
DIM1 Waveguide core width	450			480					nm	
DIM2 Waveguide gap	150								nm	
DIM3 Radius	5								um	
FUNCTIONAL At 1550nm	Specification			Extracted values					Unit	
	Min	Target	Max	Median	Mean	Std	Q90	Q10		
SPEC1 Coupling strength κ		0.1077		0.107		0.003	0.111	0.103	42	1/um
SPEC2 Coupling from 2 bend sections κ_0		0.1844		0.179		0.007	0.186	0.167	42	

4.7 Edge couplers

Representative O-Band and C-Band fiber-to-waveguide insertion loss spectrum obtained when coupling to a lensed SMF fiber and air between the SiO₂ facet and the fiber.



4.7.1 FECO_WG_SX_150

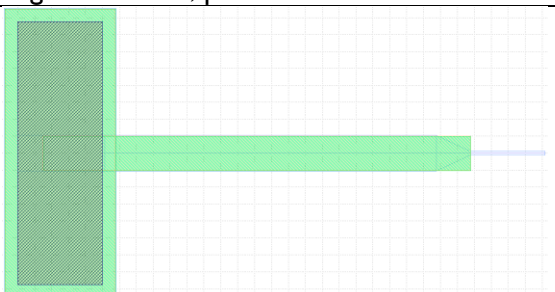
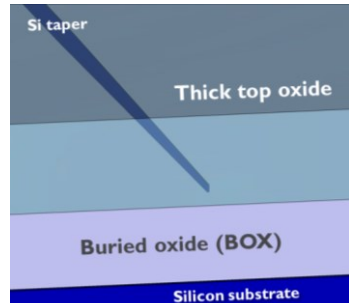
DEVICE	FECO_WG_SX_150.gds					
Family	Edge Coupler		FECO_WG_SX_150.gds			
Class	SiO ₂ inverted taper edge coupler to ~3um mode diameter		Maturity level I			
Type	High bandwidth, polarization insensitive					
GDS						
3D schematic						
STRUCTURAL		Values	Unit			
		design	Q90	Mean	Q10	
DIM1 SiO ₂ thickness above WG top surface (nominal)	2000					nm
DIM2 Silicon WG taper narrow end width (nominal)	150			155		nm
DIM3 Silicon WG taper length (nominal)	300					um

DIM4 Tip end distance to facet (nominal)	3000								nm	
DIM5 Silicon WG output width	380								nm	
DIM6 WG taper angle to facet	0								deg	
FUNCTIONAL 1300-1385nm	Specification			Extracted values (*)(**)						Unit
	Min	Target	Max	Median	Std	Q10	Q90	N	Maturity	
Minimum Insertion Loss TE				1.5					I	dB
Minimum Insertion Loss TM				3.0					I	dB
Maximum Insertion Loss TE				2.0					I	dB
Maximum Insertion Loss TM				7.5					I	dB
Maximum PDL				6.5					I	dB
FUNCTIONAL 1235-1300nm	Specification			Extracted values						Unit
	Min	Target	Max	Median	Std	Q10	Q90	N	Maturity	
Minimum Insertion Loss TE				2.0					I	dB
Minimum Insertion Loss TM				3.0					I	dB
Maximum Insertion Loss TE				4.0					I	dB
Maximum Insertion Loss TM				8.5					I	dB
Maximum PDL				6.5					I	dB

(*) Values measured on a previous version of the process. Values here only for indication, to be confirmed.

(**) Measurements have been performed with air between the SiO₂ etched facet and the fiber (lensed SMF-28 with 2.5 μm MFD @ 1310 nm).

4.7.2 FECC_WG_SX_150

DEVICE	FECC_WG_SX_150.gds												
Family	Edge Coupler			FECC_WG_SX_150.gds									
Class	SiO2 inverted taper edge coupler to ~3um mode diameter				Maturity level	I							
Type	High bandwidth, polarization insensitive												
GDS													
3D schematic													
STRUCTURAL				Values						Unit			
				design	Q10	Mean	Q90						
DIM1 SiO2 thickness above WG top surface (nominal)	2000									nm			
DIM2 Silicon WG taper narrow end width (nominal)	150			155						nm			
DIM3 Silicon WG taper length (nominal)	390									um			
DIM4 Tip end distance to facet (nominal)	3000									nm			
DIM5 Silicon WG output width	450									nm			
DIM6 WG taper angle to facet	0									deg			
FUNCTIONAL 1500-1600nm	Specification			Extracted values (*)(**)						Unit			
	Min	Target	Max	Median	Std	Q10	Q90	N	Maturity				
Minimum Insertion Loss TE				1.2					I	dB			
Minimum Insertion Loss TM				1.2					I	dB			
Maximum Insertion Loss TE				1.5					I	dB			
Maximum Insertion Loss TM				2.0					I	dB			
Maximum PDL				0.5					I	dB			

(*) Values measured on a previous version of the process. Values here only for indication, to be confirmed.

(**) Measurements have been performed with air between the SiO₂ etched facet and the fiber (lensed SMF with 2.5 μm @ 1310 nm).

4.8 Templates

When designing for a multi-project wafer (MPW) run, you choose a block size big enough to fit your layout in. To each block size corresponds a template:

Block size [μm]		TRENCH rectangle	Template cell
x	y		
2500	2500	left	TEMPLATE_2500_2500_LEFT
2500	5150	left	TEMPLATE_2500_5150_LEFT.gds
5150	2500	left, right	TEMPLATE_5150_2500.gds
5150	5150	left, right	TEMPLATE_5150_5150.gds
5150	10450	left, right	TEMPLATE_5150_10450.gds
10450	5150	left, right	TEMPLATE_10450_5150.gds
10450	10450	left, right	TEMPLATE_10450_10450.gds

All the data sent for fabrication must fit inside the polygon on the PAYLOAD layer.

To use an edge coupler it is mandatory to place it such that its TRENCH rectangle fits into one of the TRENCH rectangle of the template. For example, let's take the TEMPLATE_2500_2500_LEFT template. The user can place edge couplers as on Figure 17. Notice on Figure 18 the TRENCH rectangle of the edge coupler perfectly overlaps the TRENCH rectangle of the template in the x direction. In the y direction edge couplers must fit inside the PAYLOAD area.

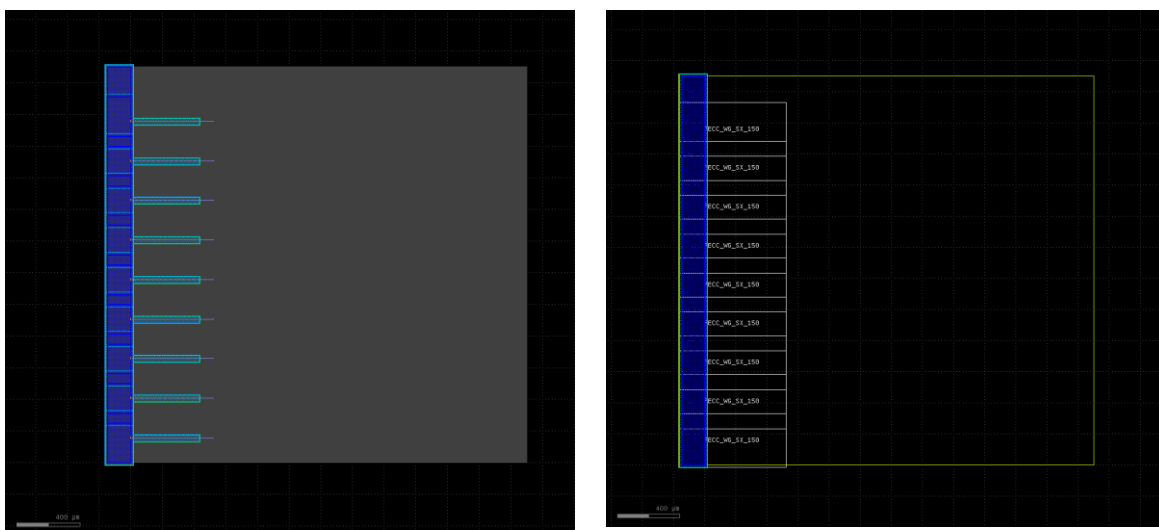


Figure 17: An example of positonning edge couplers in a TEMPLATE_2500_2500_LEFT (a) all the layers drawn (b) another view showing the template and the position of FECC_WG_SX_150 cell instances.

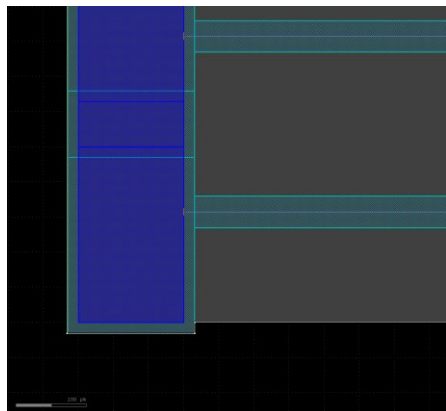


Figure 18: Detail of the placement of an edge coupler at the bottom left of Figure 17(a)

4.9 Bond pads

The ISIPP50G bond pads are carefully designed to make sure that M1 and M2 connectivity is intact. The perforations are pre-included for these two layers and via are designed not to overlap either perforations on M1 or M2, thereby ensuring a reproducible and reliable connection and device characteristics. The bond pads are 55um wide and 75 um long in the PASS1 and PASS2 layers.

Users are strongly encouraged to use this component as part of their designs and not design custom bond pads unless necessary.

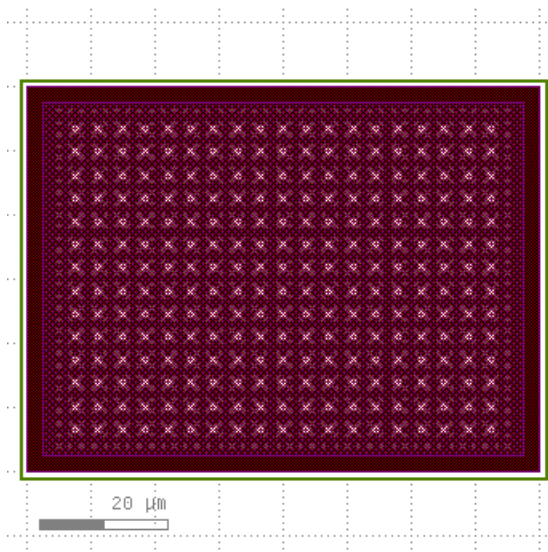


Figure 19: BP_M1M2_80_60.gds

4.10 Contacts

CONTACT_SAL.gds is designed to provide a simple mean for users for contacting the FEOL stack with the BEOL stack. The cell consists of 600 nmX600 nm SAL area over which a circular contact (W contact plug, PCON) lands. The contact plug makes contact with M1 this completing the interface from FEOL to BEOL layers.

Users must this component as part of their designs and not design custom contact plugs.

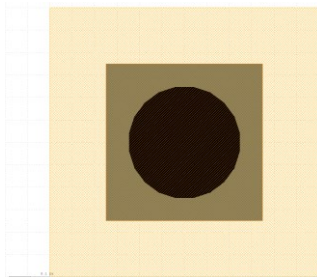


Figure 20: CONTACT_SAL.gds

4.11 50Ω Resistors

Device	Characteristic	Min	Typ	Max	Unit
RESBP_NPLUS_50	Resistance measured at 0.1V		50		Ohm

RESBP_NPLUS_50 is a 50 Ω resistor. The NPLUS area is 30μm wide and 31.2μm long. The total contact resistance (for a 0μm long resistor) is extracted to be about 2.7Ω.

A version of the device without bond pad is available as RES_NPLUS_50.gds.

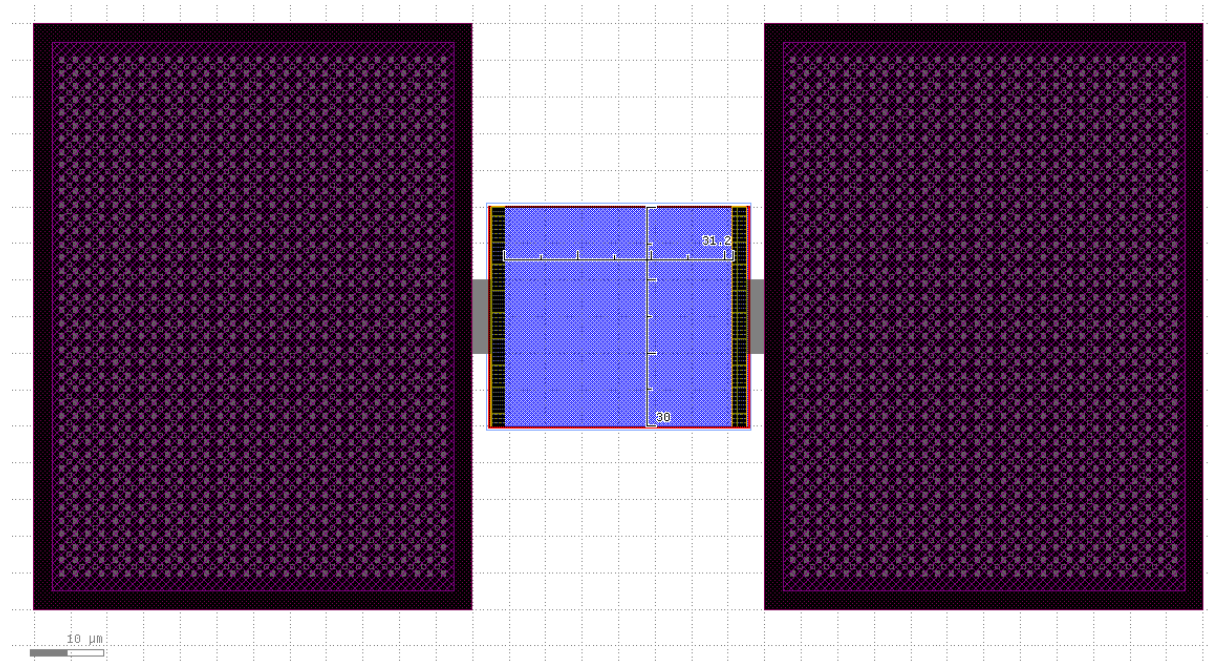


Figure 21: RESBP_NPLUS_50.gds, with bond pads

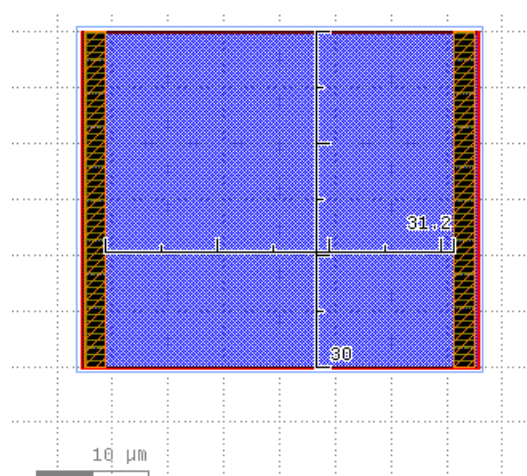


Figure 22: RES_NPLUS_50.gds, without bond pads

4.12 Doped silicon thermo-optic phase shifter

The doped silicon thermo-optic phase shift available in ISIPP50G are made of N doped sections of silicon on each side of the strip waveguide. They are available as daisy chainable cells with 200 µm long heating elements. Neither loss or phase shifter efficiency are available.



Figure 23: SWGOTE_WGNPLUS_380_600_200k.gds thermo-optic phase shifter for O-band 380 nm wide waveguide



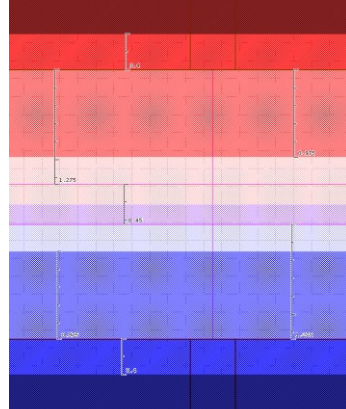
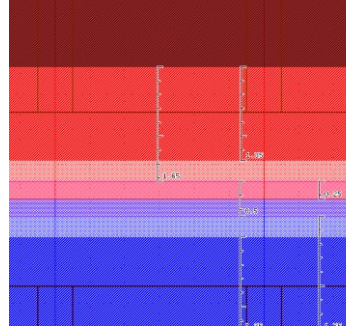
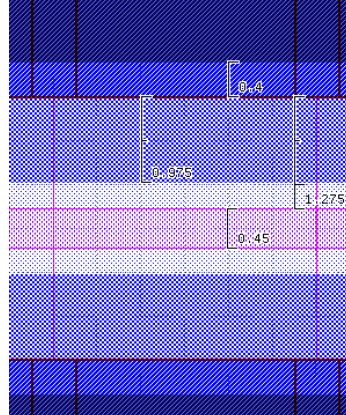
Figure 24: SWGCTE_WGNPLUS_450_600_200k.gds thermo-optic phase shifter for C-band 450 nm wide waveguide

Alternatively you can use the MH_DRW layer to draw metal heaters. The width must be 600nm.

4.13 PN depletion diode phase shifter

4.13.1 Extraction of DC resistance and capacitance

DC resistance and capacitance are measured on dedicated structures. Doping and length are changed to allow parameters extraction.

Test structure type	Layout detail
SKP1N1	
SKP2N2	
SKN1	

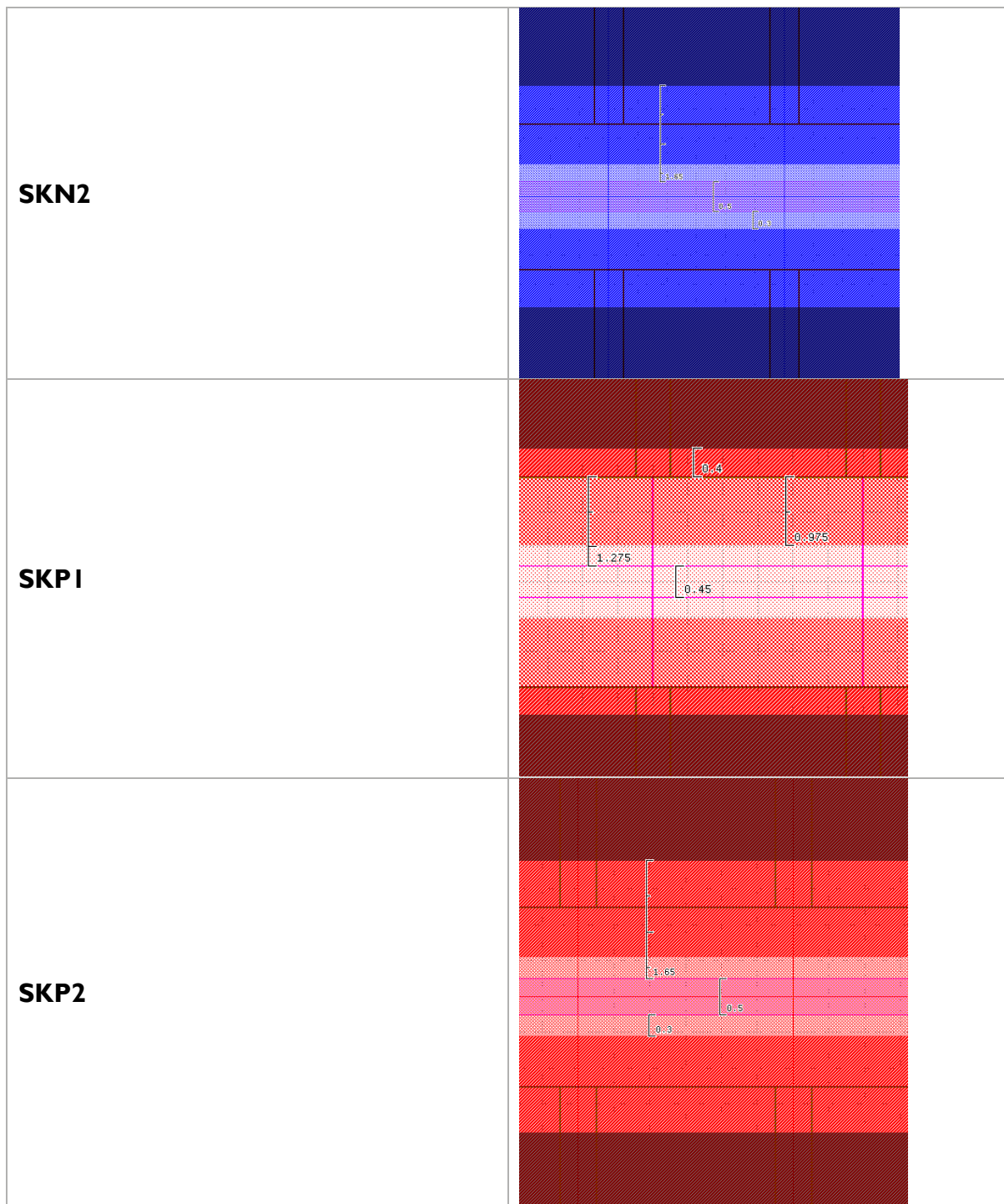


Table 1: Dimensions of test structure types

Test structure type	Length [μm]	Parameter measured	Conditions	Mean	Std Dev	Median	Q10	Q90	N
SKP1N1	48	Resistance [$\Omega \cdot \mu\text{m}$]	0.1V bias	7388	298	7415	6985	7845	24
SKP2N2	48	Resistance [$\Omega \cdot \mu\text{m}$]	0.1V bias	4415	195	4390	4160	4720	24

SKN1	48	Resistance [Ω . μ m]	0.1V bias	5188	206	5165	4890	5480	24
SKN2	48	Resistance [Ω . μ m]	0.1V bias	3521	152	3505	3300	3740	24
SKP1	48	Resistance [Ω . μ m]	0.1V bias	9601	404	9660	9010	10200	24
SKP2	48	Resistance [Ω . μ m]	0.1V bias	5311	244	5285	4990	5710	24
SKPINI	2196	Capacitance [fF/ μ m]	Vtop=0, freq=1MHz	0.323	0.0074	0.3215	0.3145	0.333	24
SKPINI	2196	Capacitance [fF/ μ m]	Vtop=-2, freq=1MHz	0.241	0.0046	0.241	0.236	0.248	24
SKPINI	492	Capacitance [fF/ μ m]	Vtop=0, freq=1MHz	0.325	0.0060	0.324	0.319	0.3355	24
SKPINI	492	Capacitance [fF/ μ m]	Vtop=-2, freq=1MHz	0.245	0.0040	0.245	0.2405	0.2515	24
SKPINI	996	Capacitance [fF/ μ m]	Vtop=0, freq=1MHz	0.331	0.0059	0.3305	0.325	0.34	24
SKPINI	996	Capacitance [fF/ μ m]	Vtop=-2, freq=1MHz	0.252	0.0039	0.252	0.248	0.258	24
SKP2N2	2196	Capacitance [fF/ μ m]	Vtop=0, freq=1MHz	0.515	0.0086	0.513	0.504	0.527	24
SKP2N2	2196	Capacitance [fF/ μ m]	Vtop=-2, freq=1MHz	0.380	0.0055	0.38	0.3735	0.3885	24
SKP2N2	492	Capacitance [fF/ μ m]	Vtop=0, freq=1MHz	0.534	0.0152	0.5335	0.5155	0.556	24
SKP2N2	492	Capacitance [fF/ μ m]	Vtop=-2, freq=1MHz	0.393	0.0091	0.3925	0.3825	0.406	24
SKP2N2	996	Capacitance [fF/ μ m]	Vtop=0, freq=1MHz	0.535	0.0147	0.533	0.517	0.556	24
SKP2N2	996	Capacitance [fF/ μ m]	Vtop=-2, freq=1MHz	0.395	0.0085	0.3935	0.385	0.407	24

4.13.2 Devices description

Reference depletion phase shifter PN diodes are provided with a lateral junction implemented in SKT rib waveguides with the N1/P1 implant conditions. The phase shifters are available as 2 sections of 500 μ m long. Both anodes must be connected together by the designer.

The 2 layouts, PSDCTE_SKPNLA_500 and PSDOTE_SKPNLA_500 differs by the width of the ridges waveguides (450nm and 380nm respectively).

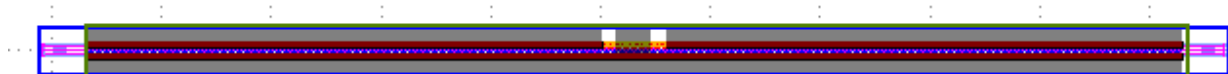


Figure 25: PSDCTE_SKPNLA_500.gds

4.13.3 Layout

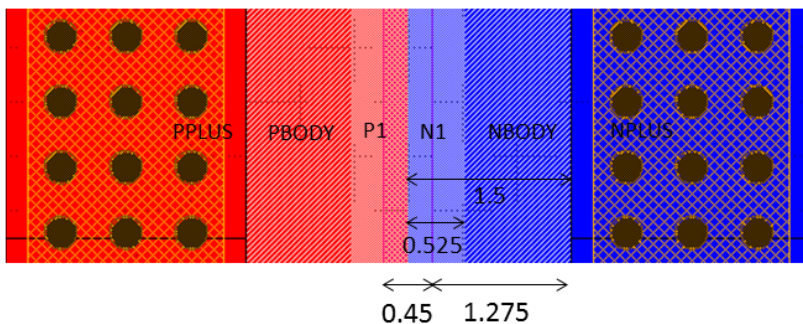


Figure 26: PSDCTE_SKPNLA reference diode layout

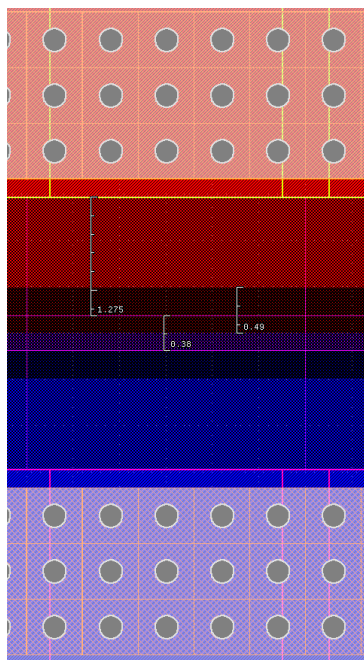


Figure 27: PSDOTE_SKNLA reference diode layout

4.13.4 Devices performance

V_{piLpi} is obtained from measuring lumped MZM having one PSD in each arm.

DEVICE	PSDCTE_SKPNLA			
Family	Depletion phase shifter			PSDCTE_SKPNLA_500.gds
Class	C-band, TE			Maturity Level 0
Type	PN diode depletion phase shifter with lateral junction			
STRUCTURAL		Values	Mean	Unit
		GDS		
DIM1 SKT waveguide width	450			nm

DIM2 SKT waveguide trench width			1275						nm	
DIM3 junction position			Center of waveguide						nm	
DIM4 NBODY distance from waveguide center			525						nm	
DIM5 NPLUS distance from waveguide center			1500						nm	
FUNCTIONAL at 1550nm										
	Min	Target	Max	Mean	Median	Std Dev	Q10	Q90	N	
Small signal V _{TH} L _{TH} at 0V				1.555	1.576	0.0844	1.424	1.655	42	V.cm
Small signal V _{TH} L _{TH} at 1V				1.711	1.728	0.0966	1.578	1.837	42	V.cm
Small signal V _{TH} L _{TH} at 2V				1.905	1.918	0.1193	1.732	2.047	42	V.cm
Optical loss at -2V				-12.2	-12.2	0.68	-13.1	-11.3	44	dB/cm
Optical loss at -1V				-12.9	-12.8	0.69	-13.8	-12.0	44	dB/cm
Optical loss at 0V				-13.8	-13.8	0.71	-14.7	-12.9	44	dB/cm

DEVICE	PSDOTE_SKPNLA										
Family	Depletion phase shifter				PSDOTE_SKPNLA_500.gds						
Class	O-band, TE				Maturity Level		0				
Type	PN diode depletion phase shifter with lateral junction										
STRUCTURAL				Values					Unit		
				GDS	Q90		Mean	Q10			
DIM1 SKT waveguide width	380								nm		
DIM2 SKT waveguide trench width	1275								nm		
DIM3 junction position	Center of waveguide								nm		
DIM4 NBODY distance from waveguide center	490								nm		
DIM5 NPLUS distance from waveguide center	1465								nm		
FUNCTIONAL at 1550nm											
	Min	Target	Max	Mean	Median	Std Dev	Q10	Q90	N		
Small signal V _{TH} L _{TH} at 0V				1.466	1.477	0.068	1.360	1.530	42	V.cm	
Small signal V _{TH} L _{TH} at 1V				1.594	1.619	0.073	1.480	1.669	42	V.cm	
Small signal V _{TH} L _{TH} at 2V				1.748	1.764	0.083	1.627	1.844	42	V.cm	
Optical loss at -2V				-12.2	-12.2	0.68	-13.1	-11.3	44	dB/cm	
Optical loss at -1V				-12.9	-12.8	0.69	-13.8	-12.0	44	dB/cm	
Optical loss at 0V				-13.8	-13.8	0.71	-14.7	-12.9	44	dB/cm	

4.14 Mach-Zehnder modulator (MZM)

The MZM in the library use diode phase shifter with the same dimensions than the PSD*TE_SKNLA above but with a different length.

4.14.1 Travelling wave, terminated

4.14.1.1 Overview

The bandwidth of travelling wave MZM can be increased by terminating the device on chip to minimize RF reflections. In this design, each signal line is terminated by two parallel n-doped silicon slabs between ground and signal. This is shown in Figure 28.

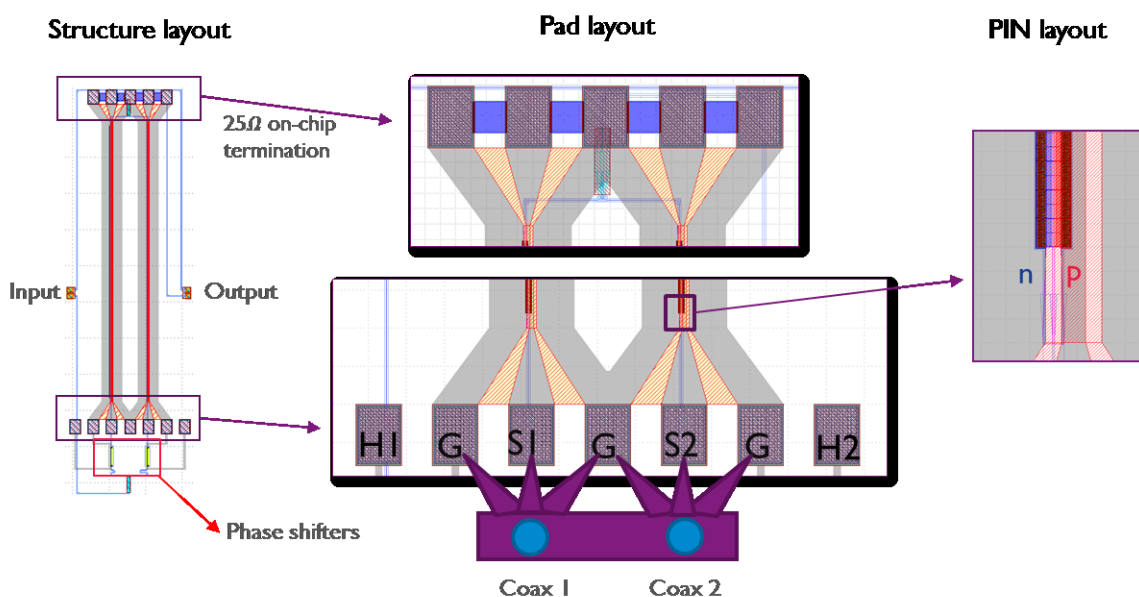


Figure 28: Design overview of the terminated travelling wave MZM

4.14.1.2 Behaviour of the termination resistors

The termination resistors are N-doped silicon resistors. Their resistance is non constant as can be seen on Figure 29.

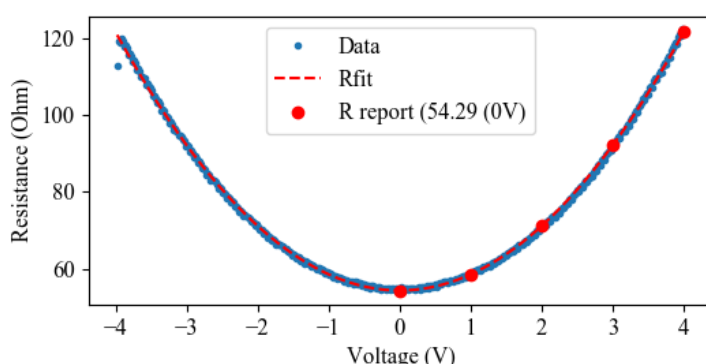


Figure 29: $R(V)$ for MZM termination resistors

4.14.1.3 Notes

- The design is available in the balanced and unbalanced version for both C and O-band. However, the analysis has been focused so far to type B, the unbalanced MZI, for C-band. However one can assume the same bandwidth for type A, and the same bandwidth for types A and B for O-band.
 - Type A: Balanced MZI (no intentional phase delay)
 - Type B: Unbalanced MZI (20um length difference)
- The names of the cells of available devices are:
 - MZMCTE_TWLAAT_450_1500.gds
 - MZMCTE_TWLAAT_450_2500.gds
 - MZMCTE_TWLADT_450_1500.gds
 - MZMCTE_TWLADT_450_2500.gds
 - MZMOTE_TWLAAT_380_1500.gds
 - MZMOTE_TWLAAT_380_2500.gds
 - MZMOTE_TWLADT_380_1500.gds
 - MZMOTE_TWLADT_380_2500.gds
- Integrated heaters can be used to tune operation wavelength. The thermo-optic V_{pi} is estimated to be 12V.
- V_{pil} has been calculated from measurements made on a lumped MZM.
- Bandwidth is extracted using S-parameters. The wavelength is set at the quadrature point.
- N1/P1 implant conditions are used.

4.14.1.4 Devices performance

DEVICE	MZMCTE_TWLADT_450_1500.gds																
Family	Mach Zehnder modulator			MZMCTE_TWLADT_450_1500.gds													
Class	Travelling wave lateral diode			Maturity level		I											
Type	Unbalanced layout – RF terminated with on-chip 25 Ohm resistance																
FUNCTIONAL																	
		Specification			Extracted values												
		Min	Target	Max	Mean	Median	Std Dev	Q10	Q90	N	Maturity						
Bandwidth 0V					24.0	24.0	1.5	22.1	25.7	46	I						
Bandwidth -1V					33.4	33.8	2.1	30.0	35.5	46	I						
Bandwidth -2V					36.8	37.2	1.2	34.7	37.8	46							

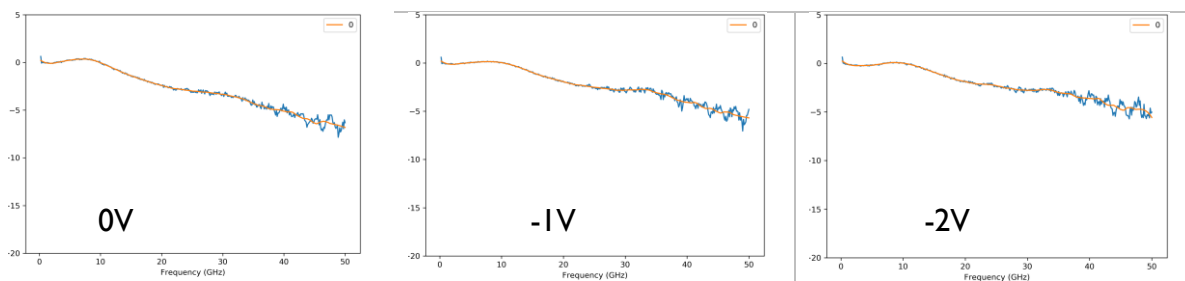


Figure 30: Typical electro-optic S21 response for the MZMCTE_TWLADT_450_1500

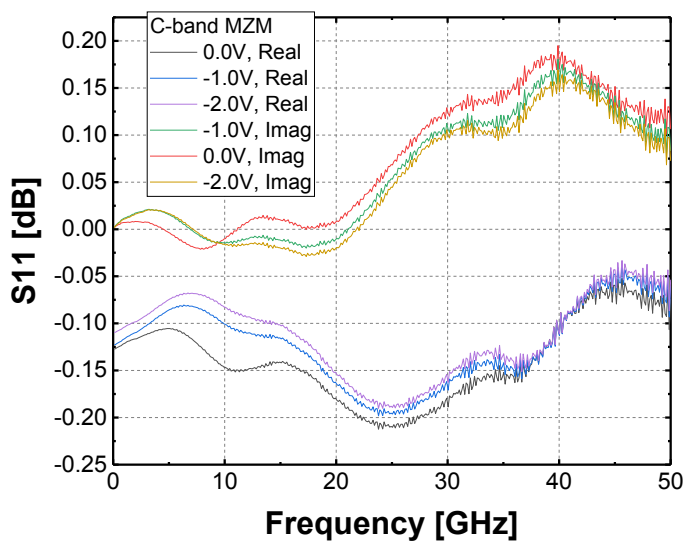


Figure 31: Typical electro-optic S₁₁ response for the MZMCTE_TWLABT_450_1500

DEVICE	MZMCTE_TWLABT_450_2500.gds								
Family	Mach Zehnder modulator	MZMCTE_TWLABT_450_2500.gds							
Class	Travelling wave lateral diode	Maturity level I							
Type	Unbalanced layout – RF terminated with on-chip 25 Ohm resistance								
FUNCTIONAL									
	Specification			Extracted values					
	Min	Target	Max	Median	Std	Q10	Q90	N	Maturity
Bandwidth 0V				15.2					0 GHz
Bandwidth -1V				18.8					0 GHz

4.15 Ring modulators

The ring modulators thereafter have been developed for high speed transmission, with bandwidth up to 50GHz for the C-band and 35Ghz for the O-band.

Their implants conditions are very different from the ones used for MZM modulators and defined with the N2/P2 modules. This allow to use both ring and MZM modulators on the same wafer without implant-related performance trade-off.

Note that, for the measurement presented thereafter, the ring modulators were connected to bond pads. The RF measurement results are presented without having de-embedded the ring modulators.

4.15.1 Thermal tuning

A metal heater is integrated above the 5 μm radius ring to tune the position of the resonance. For the O-band ring (RMOTE_SKPNLA_5000_450_140):

- Heater efficiency: 232pm/mW
- Heater power for full FSR: 58.5mW (1.7V)

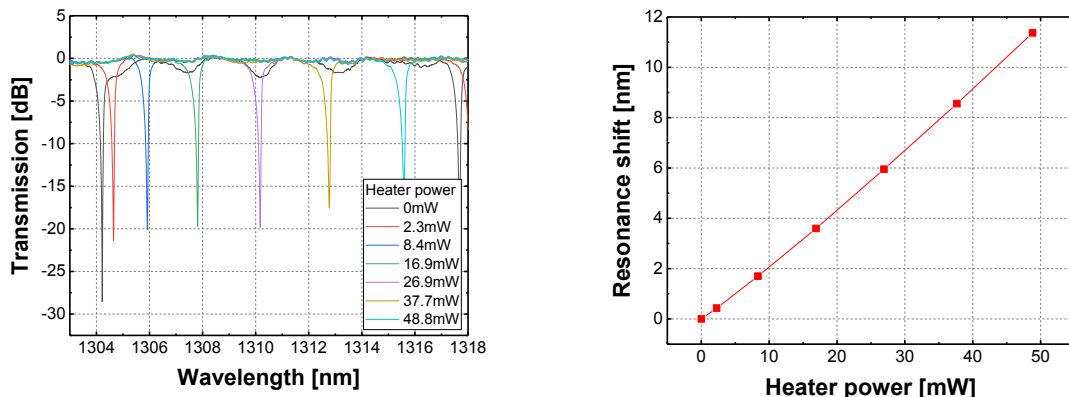


Figure 32: (left) Change in the transmission of a O-band ring for different heater power (right) Resonance shift versus heater power of the same ring

Applied voltage [V]	Heater power [mW]
0	0.0
0.25	2.3
0.5	8.4
0.75	16.9
1	26.9
1.25	37.7

1.5	48.8
-----	------

Table 2: Heater power consumed versus applied voltage for the heater of a 5 μm ring resonator

4.15.2 C-band, TE

DEVICE	RMCTE_SKPNLA_5000_500_160											
Family	Microring Modulator			RMCTE_SKPNLA_5000_500_160.gds								
Class	C-Band, TE			Maturity level		I						
Type	50G											
GDS												
STRUCTURAL				Values					Unit			
Ring Radius				5					um			
SKT waveguide width				500					nm			
Ring-Bus gap (drawn)				160					nm			
Highly doped to Waveguide edge SKT trench				750					nm			
FUNCTIONAL	Specification			Extracted values					Unit			
	Min	Target	Max	Mean	Median	Std	Q10	Q90	N	Maturity		
FSR				19.431	19.422	0.067	19.341	19.555	10	I		
ER at minTP (-1V to 0.5V)				1.8	1.7	0.1	1.7	1.9	10	I		
ER at minTP (-0.5V to 0.5V)				1.2	1.2	0.1	1.1	1.4	10	I		
IL at minTP (-1V to 0.5V)				4.9	4.9	0.05	4.8	5.0	10	I		
IL at minTP (-0.5V to 0.5V)				5.1	5.2	0.07	5.0	5.2	10	I		
Modulation efficiency (-0.5V to 0.5V)				41.4	41	4.9	37	52.9	10	I		
Modulation efficiency (-1V to 0.5V)				39.3	40	3.0	33.7	43.3	10	I		
Min Transmitter Penalty (-1V to 0.5V)				12.6	12.75	0.2	12.3	12.8	10	I		
Min Transmitter Penalty (-0.5V to 0.5V)				14.2	14.3	0.3	13.7	14.8	10	I		
calculated Q				2125	2145	60.	2031	2194	10	I		
S21 3dB Bandwidth (0V)				45.0	45.1	2.5	42.4	49.1	10	I		
S21 3dB Bandwidth (1V)				49.6	50	0.7	47.9	50	10	I		
S21 3dB Bandwidth (2V)				49.7	50	0.5	48.5	50	10	I		
										GHz		

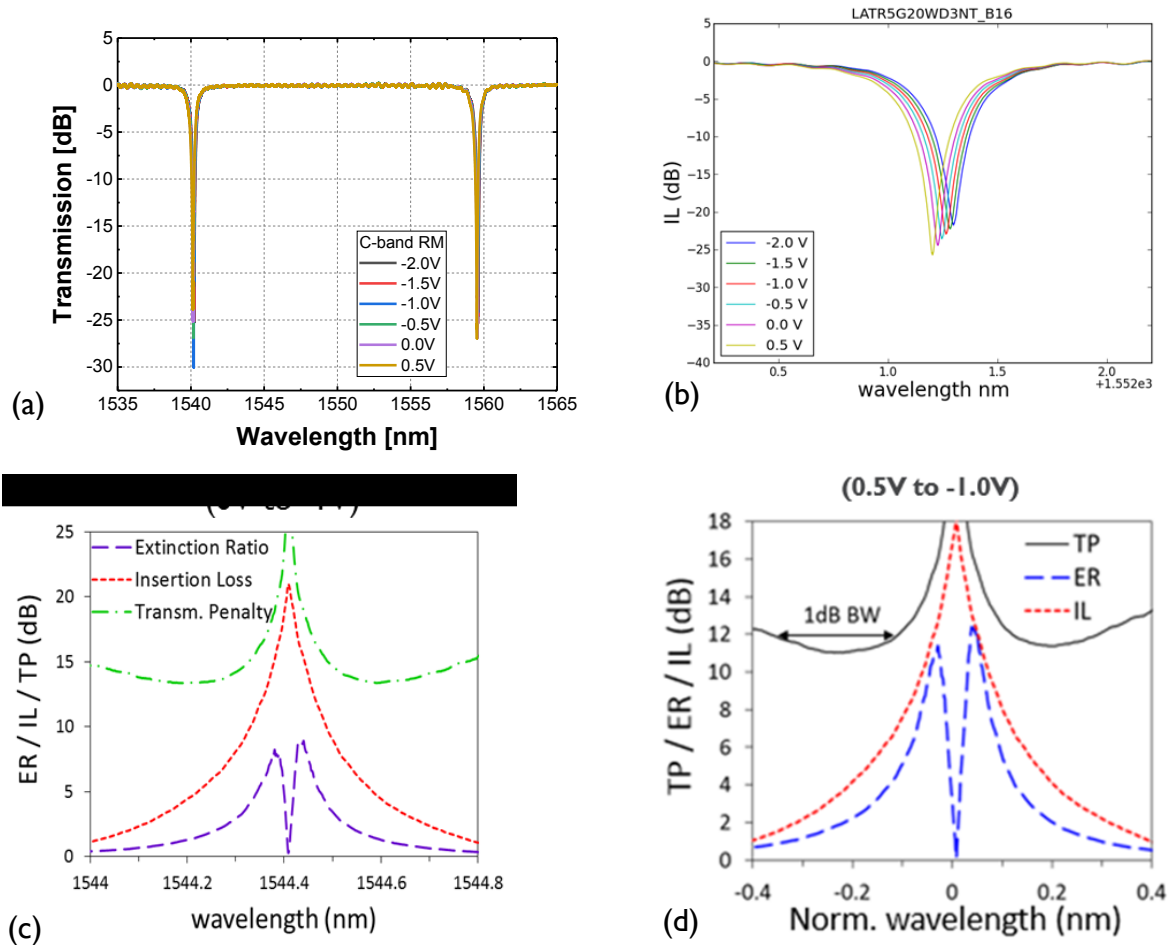


Figure 33: Typical measurements of (a) FSR (b) voltage dependent insertion loss (c) transmitter penalty (for 0 to -1V) and (d) transmssitter penalty from (0.5 to -1V).

Bias (V)	Neff	Round-trip loss	Through coefficient	Coupling coefficient
-2.0	2.680612	0.954725	0.947325	0.320273
-1.5	2.680591	0.954521	0.947592	0.319483
-1.0	2.680565	0.954268	0.947595	0.319473
-0.5	2.680534	0.953921	0.947633	0.31936
0.0	2.680503	0.953553	0.947582	0.319512
0.5	2.680466	0.953007	0.947445	0.31992

Table 3: Tabulated loss and index changes versus bias (extracted from measurements of one C-band ring)

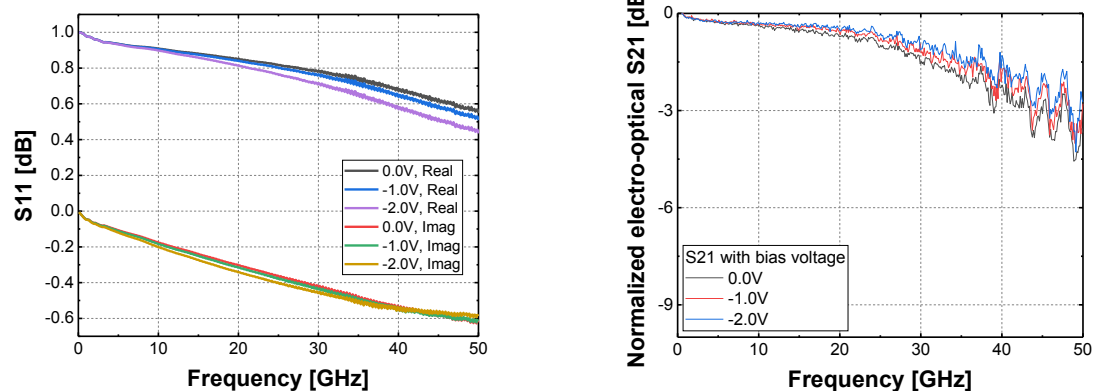


Figure 34: Typical $|S_{11}|^2$ and $|S_{21}|^2$ responses for the C-band ring modulators

4.15.3 O-band, TE

DEVICE (High Q)	RMOTE_SKPNLA_5000_450_140.gds										
Family	Microring Modulator			RMOTE_SKPNLA_5000_450_140.gds							
Class	O-Band, TE			Maturity level	I						
Type	50G										
GDS											
2D / 3D schematic											
STRUCTURAL			Values							Unit	
Ring Radius			5.0							um	
SKT waveguide width			450							nm	
Ring-Bus gap (drawn)			140							nm	
Highly doped to Waveguide SKT trench			750							nm	
FUNCTIONAL	Specification		Extracted values (*)							Unit	
	Min	Target	Max	Mean	Median	Std	Q10	Q90	N	Maturity	
FSR				13.409	13.395	0.047	13.338	13.479	11	I	
ER at minTP (-1V to 0.5V)										dB	
ER at minTP (-0.5V to 0.5V)				1.7	1.7	0.1	1.5	1.8	11	I	
IL at minTP (-1V to 0.5V)				4.6	4.6	0.1	4.4	4.7	11	I	
IL at minTP (-0.5V to 0.5V)				4.9	4.9	0.1	4.7	5.0	11	I	
Modulation efficiency (-0.5V to 0.5V)				30.5	31	1.9	27.2	33	11	I	
Modulation efficiency (-1V to 0.5V)				29.0	29.3	1.2	26.8	30.5	11	I	
Min Transmitter Penalty (-1V to 0.5V)				11.3	11.2	0.26	11.0	11.8	11	I	
Min Transmitter Penalty (-0.5V to 0.5V)				12.8	12.7	0.3	12.5	13.4	11	I	
calculated Q				3561	3642	240.7	3121	3844	11	I	
S21 3dB Bandwidth (0V)				36.6	35.3	3.9	31.1	42.3	11	I	
S21 3dB Bandwidth (1V)				39.1	39.4	4.8	33.4	47.1	11	I	
S21 3dB Bandwidth (2V)				40.8	41.4	4.1	35.1	47.1	11	I	
										GHz	

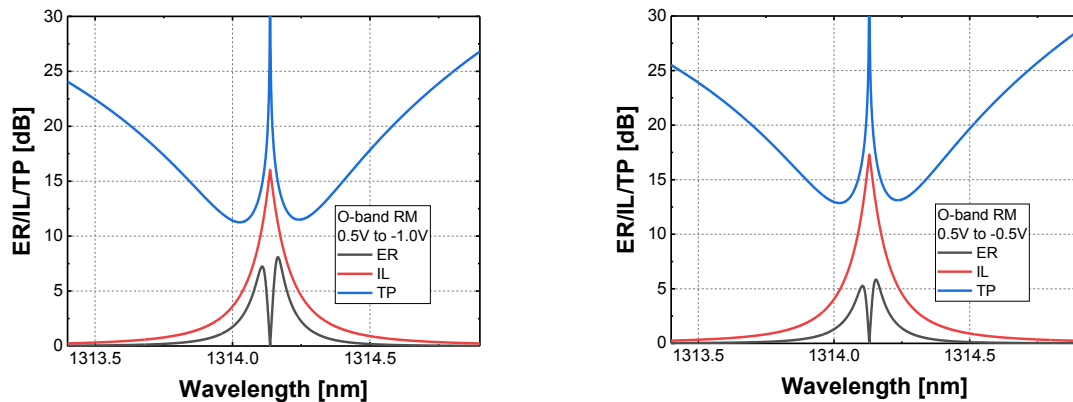


Figure 35: For O-band ring, typical measurements of (left) transmitter penalty (for 0 to -1V) and (right) transmitter penalty from (0.5 to -1V).

Bias (V)	Neff	Round-trip loss	Through coefficient	Coupling coefficient
-2.0	2.719063	0.968478	0.974219	0.225606
-1.5	2.719038	0.968419	0.974225	0.225579
-1.0	2.719013	0.968174	0.974213	0.225629
-0.5	2.718986	0.967926	0.974204	0.225669
0.0	2.718959	0.96766	0.974211	0.225638
0.5	2.718926	0.967284	0.97414	0.225944

Table 4: Tabulated loss and index changes versus bias (extracted from measurements of one O-band ring)

4.16 Ge Photodetectors

4.16.1 General information

- The photodetectors in this section are available for the Ge option only (and **not** for the SiGe option).
- The difference between C and O-band versions is in the input port width. For C-band PDs this width is 450 nm and for O-band this is 380 nm. Although these devices are optimized for TE-polarized light, one can also use those devices for TM-polarized light with typically only a slightly decreased responsivity as a consequence.
- Bandwidth is reported only for C-band TE (CTE) and is expected not to significantly change for CTM, OTE or OTM operations.
- Eye diagrams are characterized using a 44 GHz reference modulator with a 25 and 50 Gb/s 2E31-1 bit pattern (if the opto-electronic bandwidth of the device allows it). The optical power has been adjusted such that the DC current is around 300 μ A. We show only eye diagrams at -2 V and report the quality of the eye using the signal to noise ratio or SNR.
- Photodiodes building blocks should not be rotated by arbitrary angles as this adversely impacts the device performance. Only rotation by 90° and its multiples is accepted.
- Photodiodes are provided as black boxes.

4.16.2 Photodiode overview

Device name	High level properties
SVPINCFCWT_IK_15400_600	Highest bandwidth, low responsivity, low dark current at -IV
SVPINCFCWT_2K_15200_600	High bandwidth, medium responsivity, medium dark current at -IV
SVPINCFCWT_2K_13700_900	Medium bandwidth, high responsivity, low dark current at -IV
GSLPINCFCT_600_40000_450	Medium bandwidth, highest responsivity, medium dark current at -IV
SLPINCFCT_400_2000_600	Low bandwidth, highest responsivity, medium dark current at -IV

4.16.3 GPD[C/O]TE_SVPINCFCWT_IK_15400_600

DEVICE	GPD[C/O]TE_SVPINCFCWT_IK_15400_600																
Family	Germanium Photodiodes				GPD[C/O]TE_SVPINCFCWT_IK_15400_600.gds												
Class	Silicon doped vertical PIN diode				Maturity level	2											
Type	Highest bandwidth, low responsivity and low dark current																
GDS																	
STRUCTURAL				Values					Unit								
DIM1 Germanium Window Width									nm								
DIM2 Germanium Window Length									nm								
DIM3 P-contact pitch									nm								
FUNCTIONAL At 1550nm	Specification			Extracted values					Unit								
	Min	Target	Max	Median	Std	Q10	Q90	N	Maturity								
SPEC1 Responsivity CTE -IV	0.45	0.6			0.1				2	A/W							

SPEC2 Responsivity CTM -IV		0.35			0.1				2	A/W
SPEC3 Bandwidth CTE -IV	50								2	GHz
SPEC4 Bandwidth CTE -2V	50								2	GHz
FUNCTIONAL At 1310nm	Specification Extracted values									Unit
SPEC5 Responsivity OTE -IV		0.69			0.1				2	A/W
Electrical	Specification Extracted values									Unit
SPEC6 Dark current -IV		8						33	2	nA
SPEC7 Dark current -2V		50						140	2	nA

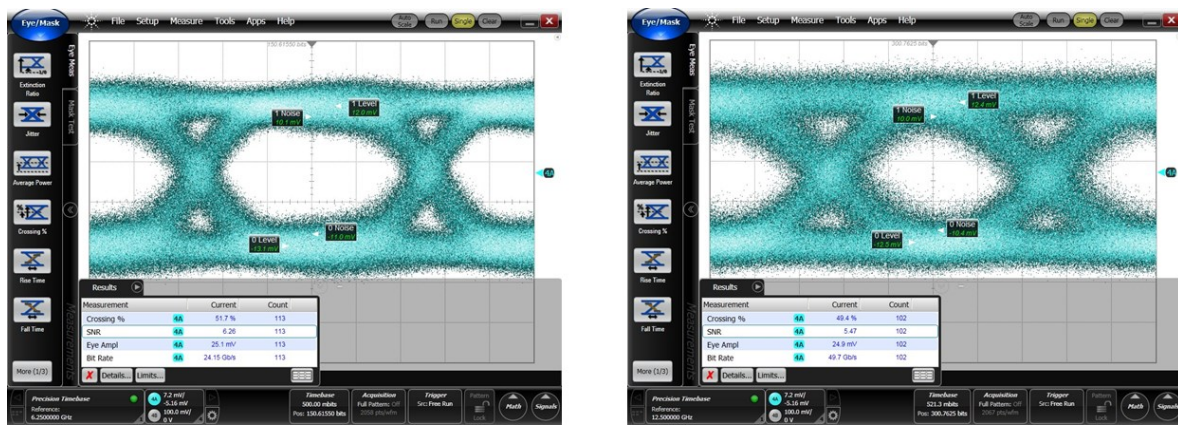


Figure 36: Eye diagrams C-band TE polarization for 25 and 50Gb/s

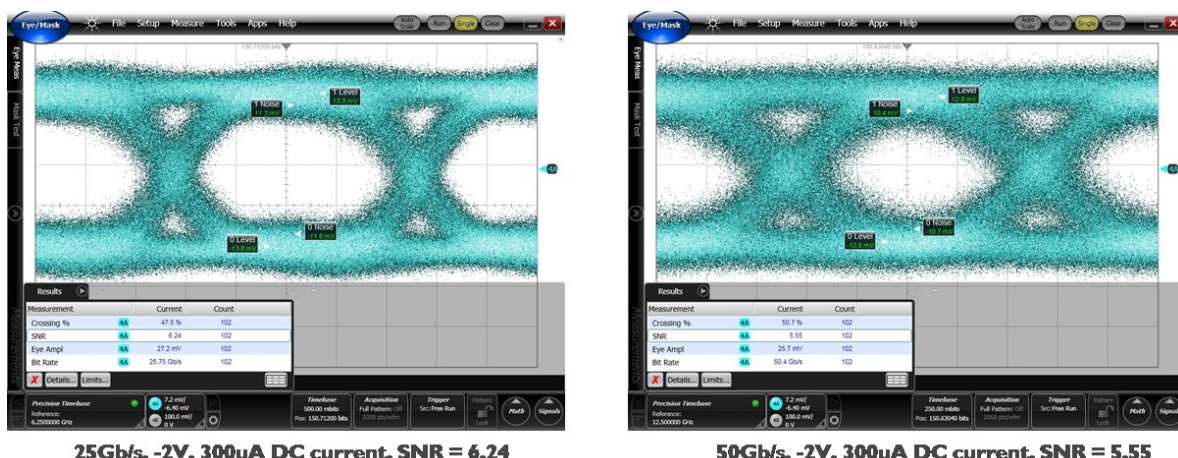


Figure 37: Eye diagrams O-band TE polarization for 25 and 50Gb/s

4.16.4 GPD[C/O]TE_SVPINCFCW_2K_15200_600

DEVICE	GPD[C/O]TE_SVPINCFCW_2000_15200_600														
Family	Germanium Photodiodes			GPD[C/O]TE_SVPINCFCW_2000_15200_600.gds											
Class	Silicon doped vertical PIN diode			Maturity level			2								
Type	High bandwidth, medium responsivity, medium dark current														
GDS															
STRUCTURAL				Values											
DIM1 Germanium Window Width															
DIM2 Germanium Window Length															
DIM3 P-contact pitch															
FUNCTIONAL	Specification			Extracted values											
At 1550nm	Min	Target	Max	Median	Std	Q10	Q90	N	Maturity						
SPEC1 Responsivity CTE -IV	0.7	0.8			0.1				2						
SPEC2 Responsivity CTM -IV		0.7			0.1				2						
SPEC3 Bandwidth CTE -IV	50								2						
SPEC4 Bandwidth CTE -2V	50								2						
FUNCTIONAL	Specification			Extracted values											
At 1310nm	Min	Target	Max	Median	Std	Q10	Q90	N	Maturity						
SPEC5 Responsivity OTE -IV		0.9			0.1				2						
Electrical	Specification			Extracted values											
	Min	Target	Max	Median	Std	Q10	Q90	N	Maturity						
SPEC6 Dark current -IV		10						31	2						
SPEC7 Dark current -2V		80						220	2						

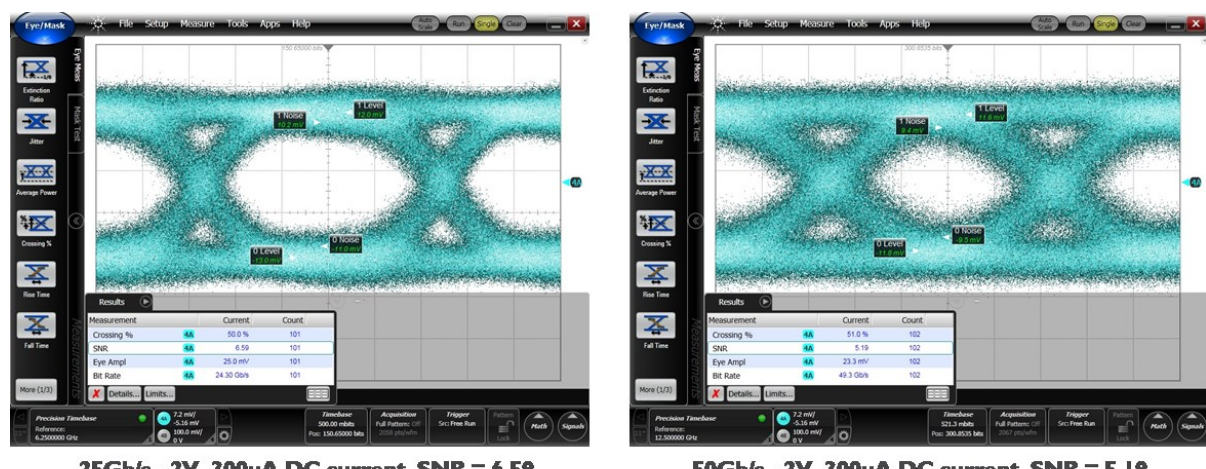


Figure 38: Eye diagrams C-band TE polarization for 25 and 50Gb/s

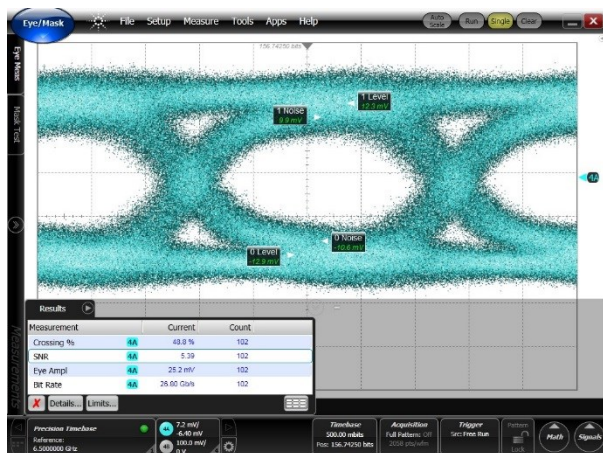


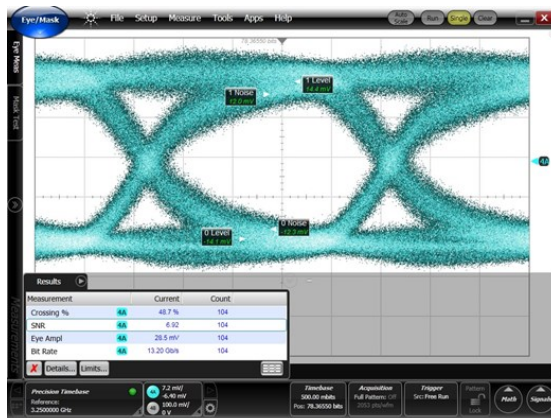
Figure 39: Eye diagrams O-band TE polarization for 25Gb/s

4.16.5 GPD[C/O]TE_SVPINDFCWT_2K_13700_900

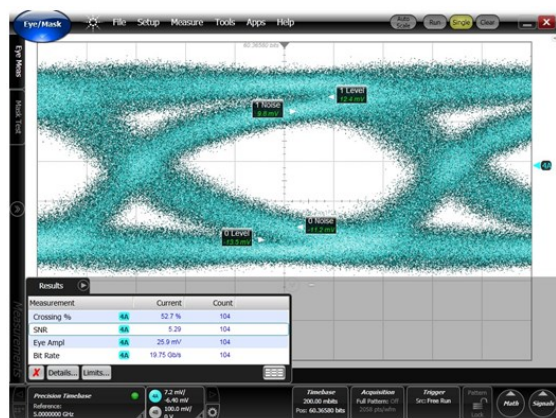
DEVICE	GPD[C/O]TE_SVPINDFCWT_2000_13700_900														
Family	Germanium Photodiodes			GPD[C/O]TE_SVPINCFCWT_2000_13700_900.gds											
Class	Silicon doped vertical PIN diode			Maturity level 2											
Type	Medium bandwidth, high responsivity, low dark current														
GDS															
STRUCTURAL				Values											
DIM1 Germanium Window Width															
DIM2 Germanium Window Length															
DIM3 P-contact pitch															
FUNCTIONAL	Specification			Extracted values											
At 1550nm	Min	Target	Max	Median	Std	Q10	Q90	N	Maturity						
SPEC1 Responsivity CTE -IV	0.75	1.0			0.1				2						
SPEC2 Responsivity CTM -IV		0.87			0.1				2						
SPEC3 Bandwidth CTE -IV	20								2						
SPEC4 Bandwidth CTE -2V	25								2						
FUNCTIONAL	Specification			Extracted values											
At 1310nm	Min	Target	Max	Median	Std	Q10	Q90	N	Maturity						
SPEC5 Responsivity OTE -IV		0.9			0.1				2						
Electrical	Specification			Extracted values											
	Min	Target	Max	Median	Std	Q10	Q90	N	Maturity						
SPEC6 Dark current -IV		10						14							
SPEC7 Dark current -2V		38						94							



Figure 40: Eye diagrams C-band TE polarization for 25 and 35Gb/s



15Gb/s, -2V, 300uA DC current, SNR = 6.92



20Gb/s, -2V, 300uA DC current, SNR = 5.29

Figure 41: Eye diagrams C-band TE polarization for 15 and 20Gb/s

4.16.6 GPD[C/O]TE_GSLPINCFWT_600_40000_450

DEVICE	GPD[C/O]TE_GSLPINCFWT_600_40000_450																		
Family	Germanium Photodiodes			GPD[C/O]TE_GSLPINCFWT_600_40000_450.gds															
Class	Ge & Si doped lateral PIN diode			Maturity level		I													
Type	Medium bandwidth, highest responsivity, medium dark current																		
GDS																			
STRUCTURAL				Values															
DIM1 Intrinsic diode width																			
DIM2 Germanium window length																			
DIM3 Germanium window width																			
FUNCTIONAL	Specification			Extracted values															
At 1550nm	Min	Target	Max	Median	Std	Q10	Q90	N	Maturity										
SPEC1 Responsivity CTE -IV	0.8	1.1			0.1				I										
SPEC2 Responsivity CTM -IV		0.78			0.1				I										
SPEC3 Bandwidth CTE -IV	25	33							I										
SPEC4 Bandwidth CTE -2V	30	42							I										
FUNCTIONAL	Specification			Extracted values															
At 1310nm	Min	Target	Max	Median	Std	Q10	Q90	N	Maturity										
SPEC5 Responsivity OTE -IV		0.9			0.1				I										
Electrical	Specification			Extracted values															
	Min	Target	Max	Median	Std	Q10	Q90	N	Maturity										
SPEC6 Dark current -IV		20					20		I										
SPEC7 Dark current -2V		200					250		I										

4.16.7 GPD[C/O]TE_SLPINCFCT_400_20800_600

DEVICE	GPD[C/O]TE_SLPINCFCT_400_20800_600																	
Family	Germanium Photodiodes			GPD[C/O]TE_SLPINCFCT_400_20800_600.gds														
Class	Si doped lateral PIN diode			Maturity level		2												
Type	Low bandwidth, highest responsivity, low dark current																	
GDS																		
STRUCTURAL				Values														
DIM1 Intrinsic diode width																		
DIM2 Germanium window length																		
DIM3 Germanium window width																		
FUNCTIONAL	Specification			Extracted values														
At 1550nm	Min	Target	Max	Median	Std	Q10	Q90	N	Maturity									
SPEC1 Responsivity CTE -IV	0.85	1.1			0.1				2									
SPEC2 Responsivity CTM -IV									A/W									
SPEC3 Bandwidth CTE -IV		7							GHz									
SPEC4 Bandwidth CTE -2V		17							GHz									
FUNCTIONAL	Specification			Extracted values														
At 1310nm	Min	Target	Max	Median	Std	Q10	Q90	N	Maturity									
SPEC5 Responsivity OTE -IV		0.8			0.1				I									
Electrical	Specification			Extracted values														
	Min	Target	Max	Median	Std	Q10	Q90	N	Maturity									
SPEC6 Dark current -IV		5					8		2									
SPEC7 Dark current -2V		50					110		2									
									nA									

4.17 SiGe devices

4.17.1 General information

The devices described hereafter are only available with the SiGe process option. They are aimed at high speed C-band operation.

4.17.2 EAM

DEVICE	EAMCTE_GSLPINCFWT_600_40000_450.gds									
Family	Germanium EAM			EAMCTE_GSLPINCFWT_600_40000_450.gds						
Class	C-band, TE			Maturity level	I					
Type										
STRUCTURAL				Values					Unit	
Footprint									µm ²	
FUNCTIONAL at 1550 nm with a voltage swing of 2.0V										
	Specification			Extracted values						
	Min	Target	Max	Median	Std	Q10	Q90	N	Maturity	
SPEC1 Optical bandwidth		30							I	nm
SPEC2 ER		3.4							I	dB
SPEC3 IL		6							I	dB
SPEC4 Static power consumption		1.7							I	mW
SPEC5 Dynamic power consumption		13.8							I	fJ/bit
SPEC6 3db Bandwidth	50								I	GHz
SPEC7 Max. Bit rate		56							I	Gb/s
SPEC 8 Responsivity		0.65							I	A/W
SPEC 9 Dark Current		200							I	nA

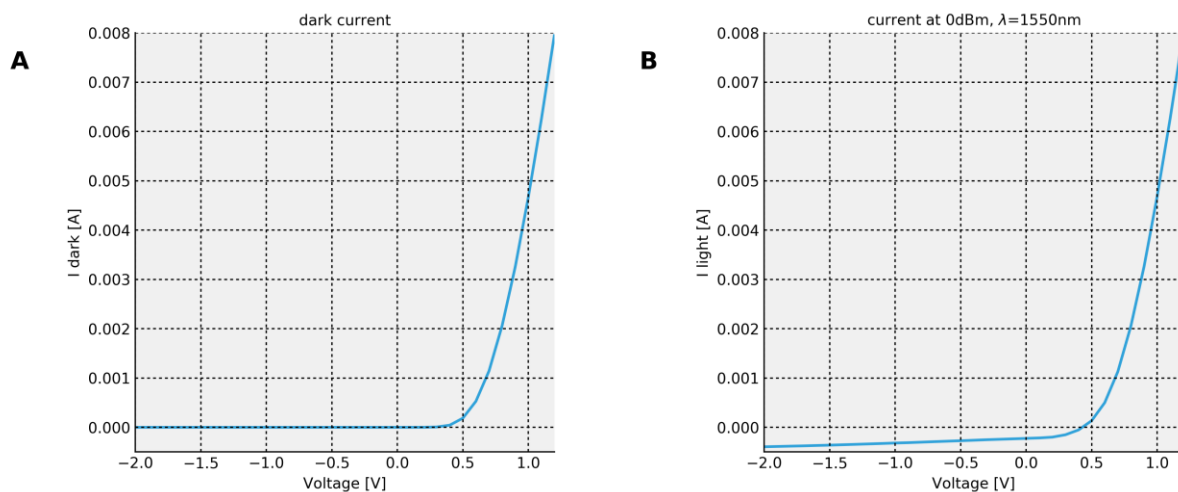


Figure 42: (A) I-V without illumination (B) I-V under 0dBm of light @ 1550nm

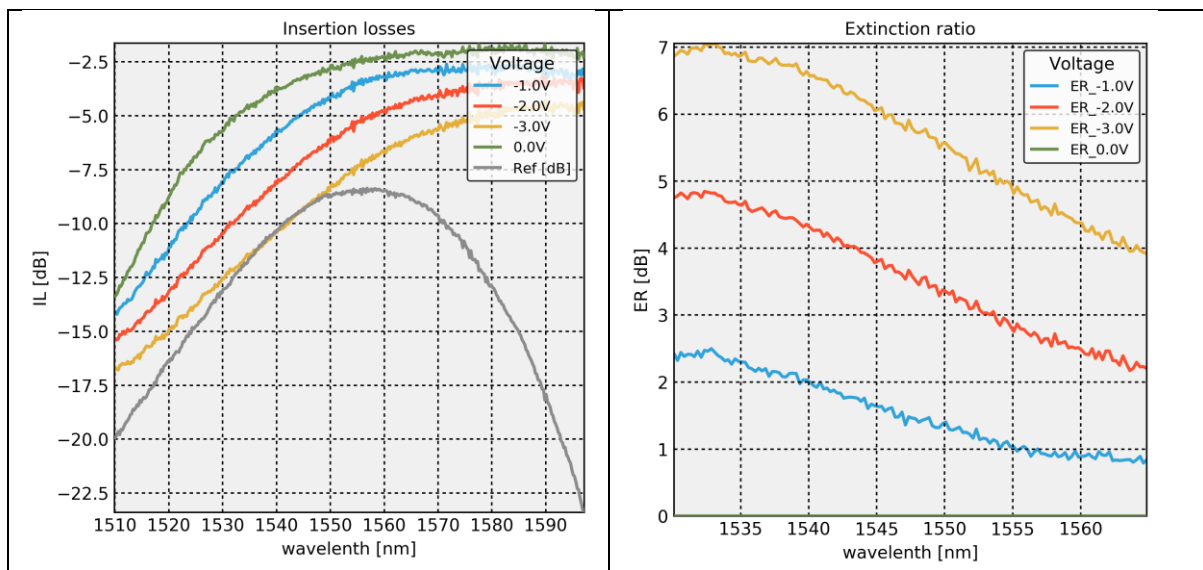


Figure 43: (left) insertion losses (right) extinction ratio. Both with 0dBm of light at DUT.

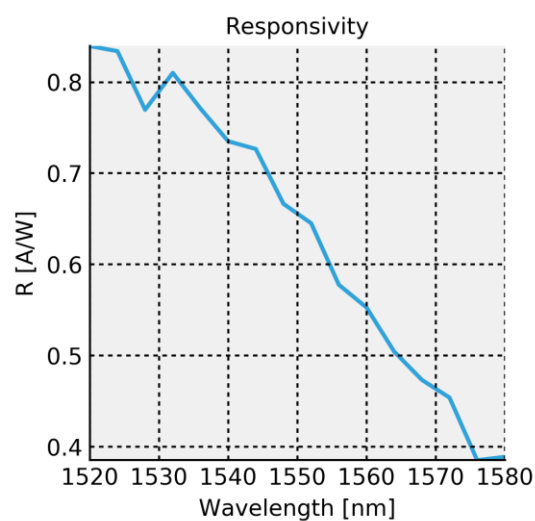


Figure 44: Responsivity vs. wavelength at -1.2V

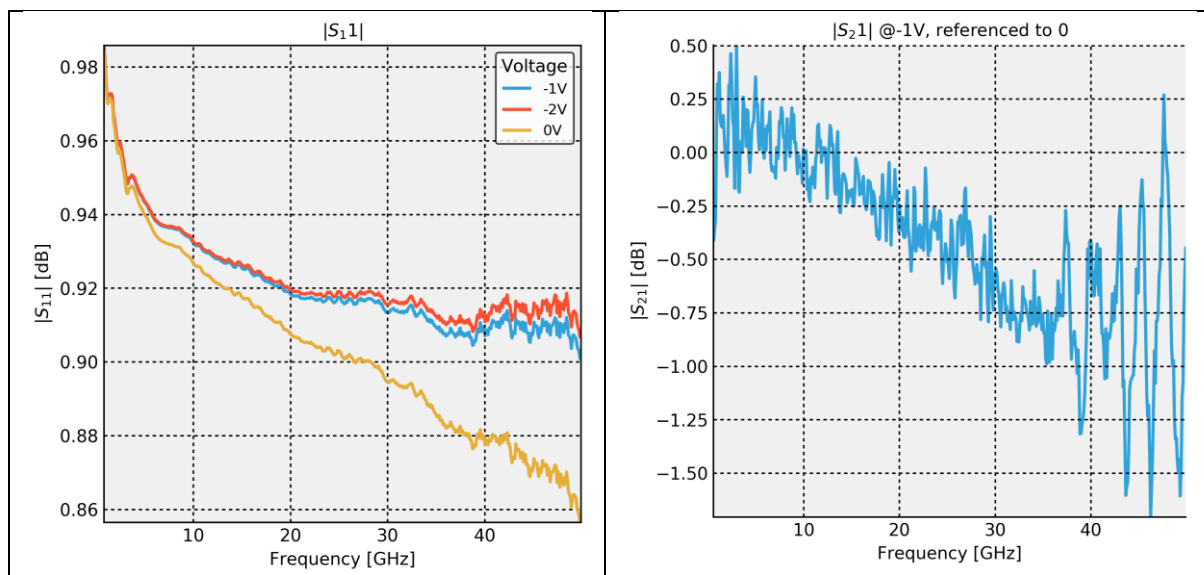


Figure 45: (left) RF S_{11} measurements at 0, -1 and -2V. (right) RF S_{21} measurement at -1V referenced to 0.

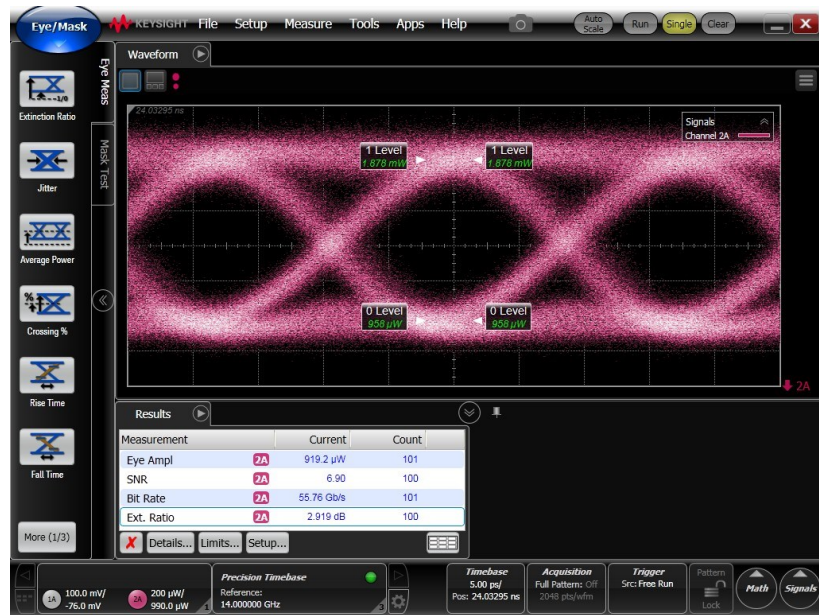


Figure 46: Eye diagram at 56Gbit/s., with PRBS2e-31, 2dBm power at DUT, voltage range 0 to 2V.

4.17.3 Photodetector GPDCTE_GSLPINCFWT_500_81600_350

GPDCTE_GSLPINCFWT_500_81600_350 is a SiGe-based photodetector that can be used together with the EAM

DEVICE	GPDCTE_GSLPINCFWT_500_81600_350																			
Family	Germanium Photodiodes			GPDCTE_GSLPINCFWT_500_81600_350.gds																
Class	SiGe lateral PIN diode			Maturity level		I														
Type	High bandwidth, high responsivity, low dark current																			
GDS																				
STRUCTURAL				Values						Unit										
DIM1 Intrinsic diode width										nm										
DIM2 Germanium window length										nm										
DIM3 Germanium window width										nm										
FUNCTIONAL At 1550nm	Specification			Extracted values						Unit										
	Min	Target	Max	Median	Std	Q10	Q90	N	Maturity											
SPEC1 Responsivity CTE -IV		0.8								A/W										
SPEC2 Responsivity CTM -IV										A/W										
SPEC3 Bandwidth CTE -IV	50									GHz										
SPEC4 Bandwidth CTE -2V	50									GHz										
FUNCTIONAL At 1310nm	Specification			Extracted values						Unit										
	Min	Target	Max	Median	Std	Q10	Q90	N	Maturity											
SPEC5 Responsivity OTE -IV										A/W										
Electrical	Specification			Extracted values						Unit										

	Min	Target	Max	Median	Std	Q10	Q90	N	Maturity	
SPEC6 Dark current -1V		40								nA
SPEC7 Dark current -2V		400								nA

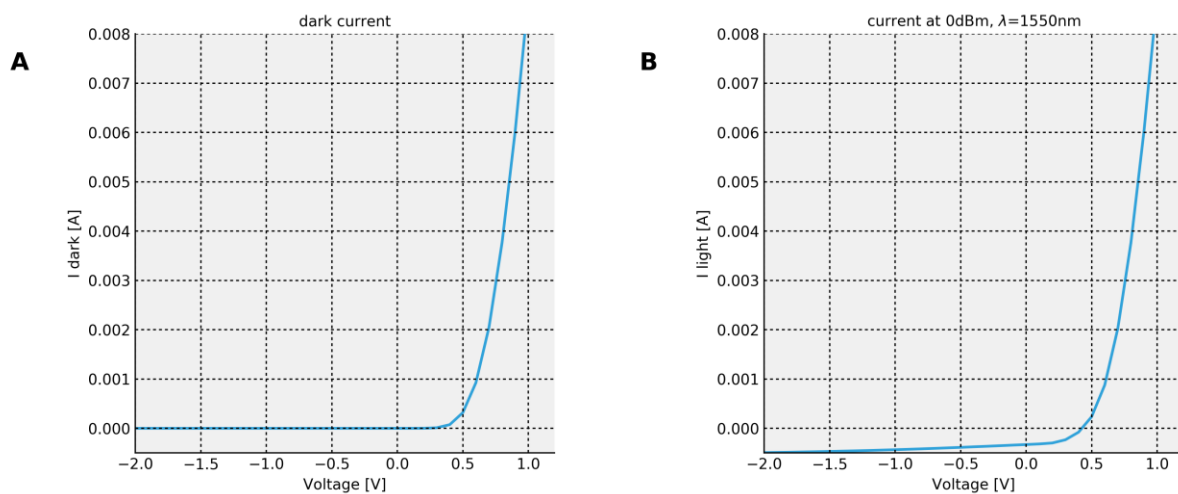


Figure 47: (A) I-V without illumination (B) I-V under 0dBm of light @ 1550nm

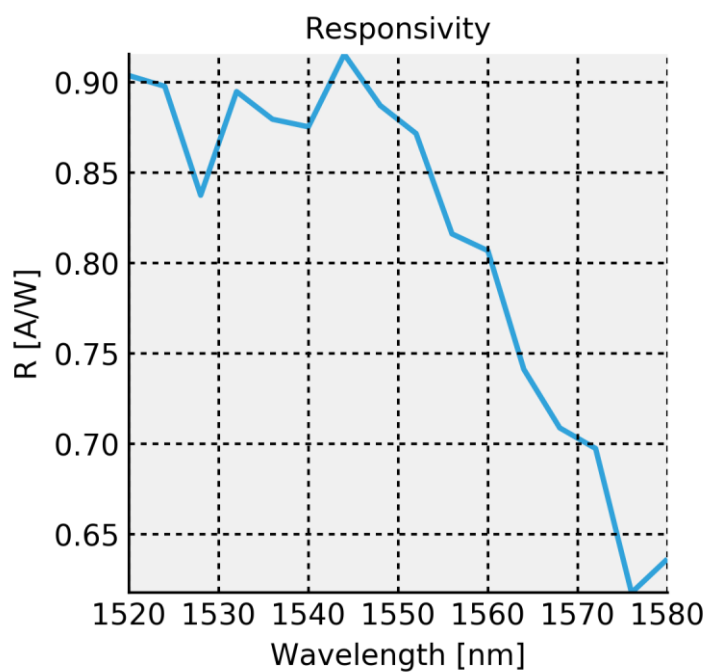


Figure 48: Responsivity vs. wavelength at -1.2V

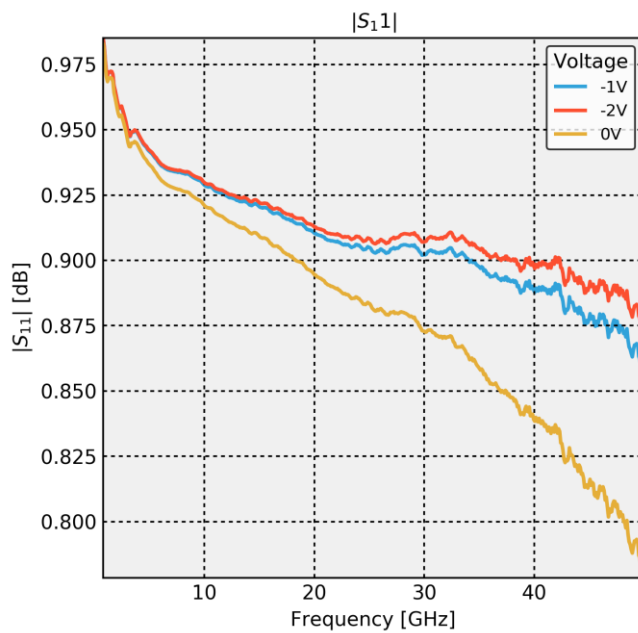


Figure 49: RF SII measurements at 0, -1 and -2V





Figure 50: Eye diagrams at 25, 30, 40, 50 and 56Gbit/s with a bias of -1 or -2V. PRBS 2e-31. @1565nm.